9 772723 437005

Telkom University
Jl. Telekomunikasi 1 Terusan Buah Batu, Bandung, Provinsi Jawa Barat, 40257
Email: journals@telkomuniversity.ac.id
Web: journals.telkomuniversity.ac.id/complete

COMPLETE | Journal of Computer, Electronic, and Telecommunication | Vol. 5 No. 2 December 2024

COMPLETE

Journal of Computer, Electronic, and Telecommunication

Vol. 5 No.2 December 2024

JURNAL

KEMAJUAN TEKNIK KOMPUTER, ELEKTRO, & TELEKOMUNIKASI

ISSN: 2723-4371 E-ISSN: 2723-5912

Telkom University

Website: journals.telkomuniversity.ac.id/complete | Email: journals@telkomuniversity.ac.id

EDITORIAL TEAM

Journal of Computer, Electronic, and Telecommunication

Telkom University

Ketintang Str. No. 156, Surabaya, 60231, East Java, Indonesia

E-mail: complete@ittelkom-sby.ac.id;

Web: journal.ittelkom-sby.ac.id/complete

(This page is intentionally left blank)

TABLE OF CONTENTS

(This page is intentionally left blank)

ABOUT THE JOURNAL

COMPLETE : Journal of Computer, Electronic, and Telecommunication is an official journal of Telkom University. It publishes research or review articles in Computer, Electronic, and Telecommunication technology. This journal provides a platform for research lecturers, reviewers, practitioners, industry, and observers across Indonesia and overseas to promote, share, and discuss new issues and technology development. The scope of the journal includes:

- Technology utilization of maritime resources
- Strengthening infrastructure maritime
- Technology and management safety transportation
- Industrial strengthening technology transportation
- Supporting infrastructure and transportation system
- Operational efficiency
- Electronics Technology
- Telecommunication Technology
- Computer Technology
- System Security
- Advanced Robotics Technology
- Technology and disaster management
- Advanced Power Electronics
- Application of Power System
- Renewable Energy
- Chips Technology
- Sensor Technology
- Smart IoT Devices
- 5G Technology and Ecosystems
- Technology and management environment

COMPLETE published twice a year. Editors invite research lecturers, the reviewer, practitioners, industry, and observers to contribute to this journal. The language used in the form of Indonesian and English. All accepted manuscripts will receive individual digital object identifier (DOI) and indexed by Sinta, Arjuna, and Google Scholar. The online PDF version of the journal is open access from journal.ittelkom-sby.ac.id/complete. Subscription of the hard copy can be requested by email to complete@ittelkom-sby.ac.id.

(This page is intentionally left blank)

PREFACE

Welcome to the Journal of Computer, Electronic, and Telecommunication, Vol. 5, Issue No. 2. It is my privilege and pleasure to present the fifth volume of this peer-reviewed journal under Telkom University. This journal aims to accommodate the results of research publications through national and worldwide journals as part of continuous improvement.

As the chairman of COMPLETE, I would like to thank many people who supported this journal, especially Research and Community Service Units (LPPM). Furthermore, as the editor-in-chief, I would like to extend my sincere thanks to all members of the editorial and the advisory boards from Telkom University, whose service, dedication, and commitment have made the creation of this journal possible. We work together to improve the quality and excellence of articles published continuously.

We hope that COMPLETE could deliver valuable and interesting information and stimulate further research to the worldwide telecommunications, electrical, and computer engineering communities.

Surabaya, December 2024

Editor-In-Chief of Journal

(This page is intentionally left blank)

COMPLETE
Journal of Computer, Electronic, and Telecommunication
ISSN 2723-4371, E-ISSN 2723-5912

Article

Sign Language Detection Based on EMG and IMU Sensors Using Neural Network

Muhammad Nur Al Majid [1], Mas Aly Afandi [2] and Sevia Indah Purnama [3*]

[1] Electrical Engineering Study Program, Universitas Telkom, Banyumas, Indonesia
[2, 3] Center of Excellence Healthcare and Wellbeing Technology, Universitas Telkom, Banyumas, Indonesia

* Correspondence: seviaindah@telkomuniversity.ac.id

Received: 19 November 2024; Revised: 28 November 2024; Accepted: 31 December 2024

Abstract: Sign language is a way of communication for people with hearing and speech impairments. Sign language is generally done using hand gestures to articulate sentences. Different countries use different sign languages, increasing the complexity of sign language recognition. Communication between non-disabled and disabled people is difficult because non-disabled people do not learn sign language. This research aims to develop a device that can translate sign language specific to telling body conditions so that people without disabilities can understand. The device uses sensors to determine hand movement patterns to recognize sign language. The sign language recognized in this study focuses on body conditions and diseases such as asthma, cough, dizziness, depression, and tonsils. The results of the test show that the Artificial Neural Network (ANN) model has good performance with 98% accuracy value, 98% precision value, 98% recall, and 98% F1-Score. The test was conducted after the model was implanted and used to perform sign language testing. The parameter value of the confusion matrix shows high results. It can be concluded that the model created can be used to translate sign language to express the condition of tonsils, cough, depression, dizziness, and asthma.

Keywords: Artificial Neural Network, Disabilities, Sign Language

1. Introduction

Based on records released by the Badan Pusat Statistik (BPS) in 2020, there were 22.5 million people with disabilities in Indonesia. The largest group of people with functional disabilities in Indonesia, namely people with severe disabilities, with a total of 6.1 million people, which includes 1.2 million people with physical limitations, 3.07 million people with sensory limitations, 149,000 people with mental limitations, and 1.7 million people have intellectual disabilities [1].

Based on the survey results regarding the rights of persons with disabilities as stipulated in Law Number 8 of 2016 and Government Regulation Number 70 of 2019 concerning Planning, Implementation, and Evaluation of Respect, Protection and Realization of the Rights of Persons with Disabilities needs to be improved. The fulfilment of rights that are not maximized will cause various risks ranging from socioeconomic inequality and limitations on access to information, employment, health, education, and other issues compared to normal citizens [2]. Different types of people with disabilities have different needs. Based on data from BPS in 2020 states that the rate of speech disorders reached 0.35 per cent and hearing impairment reached 0.36 per cent [3]. People with speech and hearing impairments use the same method of communication, namely hand sign language.

Hand sign language is a language that is often used to help people with disabilities communicate. Sign languages that are often used are Bahasa Isyarat Indonesia (BISINDO) and Sistem Bahasa Isyarat Indonesia (SIBI). This sign language was developed directly by people with

disabilities [4]. However, not everyone understands sign language, so there is often a communication gap that complicates between people with hearing and speech impairments and normal citizens. So that there is a misunderstanding or lack of information conveyed properly between sign language users and people who do not understand sign language [5]. This results in economic, social, and other access inequalities. Research about sign language recognition using a sensor is has high interest since so many disabled people. Research [6]–[8] discusses the use of EMG and IMU sensors to translate sign language into American and Persian. Sign language in unique and different countries has different gestures. This research aims to develop a sign language recognition device to translate Indonesian sign language. The device focuses on recognizing sign language to tell the body condition specific to hand gestures. The health conditions examined in this research include tonsillitis, cough, depression, dizziness, and asthma. These conditions are commonly encountered in everyday life and frequently arise in conversations. Understanding these health issues can help the general public recognize the challenges faced by individuals with disabilities in both school and workplace settings.

The large number of people who use sign language and have similar needs form the basis of the importance of developing a sign language translation device. In order to improve the accessibility of communication between individuals in normal conditions and people with disabilities, it is necessary to develop a device that is able to interpret sign language. With this sign language interpretation facility, it is expected that there will be a significant improvement in the ability to communicate effectively between people with disabilities and non-disabled people.

2. Methods

The research consisted of hardware and software system development. The hardware is used to measure the arm position and muscle signals when sign language is performed. The software is used to run the pre-trained model to recognize the sign language being performed. The final output of the developed device is a voice that provides information on the sign language performed. The study recognized 5 sign languages that indicate health, namely tonsils, asthma, cough, depression and headache.

2.1 Hardware System

The hardware is developed using sensors, microcontrollers, and actuators. Sensors are used to record changes that occur in hand position and muscle signals when performing sign language. The microcontroller is used to process the data that has been recorded by the sensor and send control signals to the actuator. Actuators are used to provide sign language information that is being performed by people with disabilities.

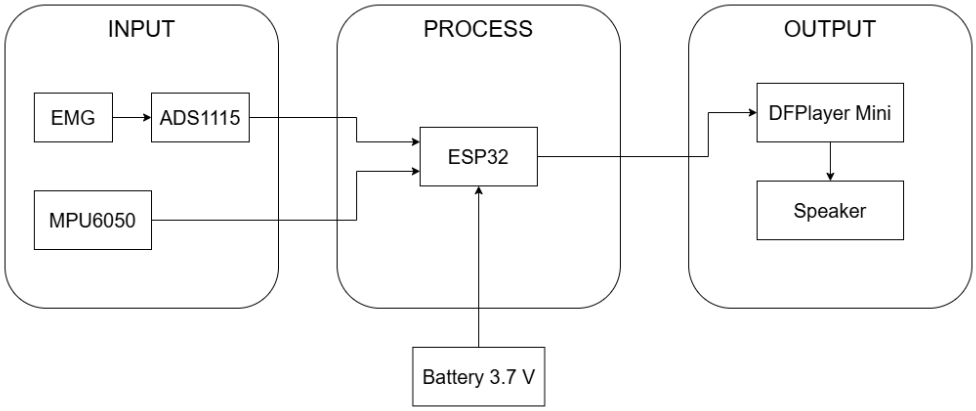

Figure 1. Hardware System Block Diagram

Figure 1 shows that the developed sign language translation device uses an esp32 microcontroller, EMG sensor, ADS1115 device, MPU6050 sensor, DFPlayer Mini, and speaker with a 3.7 volt battery power supply. The characterization pattern used to develop the translator device is the position characteristic recorded using the MPU6050 sensor. This sensor is able to provide position data in 3-dimensional space so that the position of the hand when translating sign language can be known [9]. This research also utilizes muscle signal features during sign language. The combination of hand location features and muscle strength used during sign language is a pattern that will be recognized using the neural network method. The ADS1115 device is used to convert analogue signals on EMG sensors into digital values. This tool is needed because the Analog Digital Converter (ADC) system on the ESP32 microcontroller has many quantization errors [10]. The digital data on the MPU6050 sensor and the muscle signal will be the input processed by the ESP32 microcontroller. The ESP32 microcontroller is used because it has a larger memory, which allows it to load the neural network model developed [11]. The result of the processing is a classification of the conditions of tonsils, asthma, cough, depression, and headache. The condition will be issued in the form of sound by the speaker so that the intentions of people with disabilities can be known by communication opponents who do not have disabilities.

2.2 Software System

The software system development in this research consists of the training process and the overall system performance software. Artificial Neural Network (ANN) is a type of machine learning used to model sign language translators. ANN is a data processing system inspired by the way the human brain works, consisting of interconnected processing units, such as neurons. Through the adjustment of weights and activation functions, ANN processes information to learn and adapt itself based on the given data [12].

Figure 2 is the architecture used to develop the sign language translator model in this study. The input used consists of 4 data, namely EMG, Pitch, Roll, and Yaw, which represent the movement and angle of the hand. There are 2 layers used in this research. The first layer consists of 50 neurons using the activation of each neuron in the form of relu, while the second layer consists of 25 neurons using the same activation in the form of relu. Relu activation is an activation function that will map the x value if x> 0. If the x value is a negative value, it will be converted to 0 [13]. The output part of the model consists of 5 classes (tonsils, asthma, cough, depression and headache) using softmax activation. Softmax activation is another form of Logistic Regression that can be used to classify more than two classes. This activation is used to transform the output of the last layer into its underlying probability distribution. Softmax activation calculates the probability for each class and then converts the vector of real values into a range between zero and one so that when summed up, they will all be worth one [14].

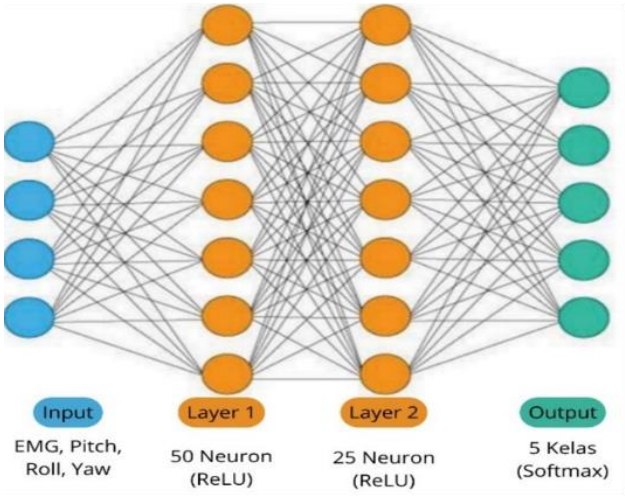

Figure 2. Artificial Neural Network (ANN) Architecture

2.2.1 Dataset Collection

Datasets are structured and organized collections of data used to train and test machine learning models in pattern recognition or classification. In this research, the dataset contains gesture data representing various disease classes, which are used to train a machine learning-based sign language interpreter model [15]. The dataset used in this research acts as the main component in the development of the machine learning-based sign language interpreter system. Dataset collection is done with the aim of obtaining representative data from various gestures that represent certain disease classes. The collected dataset has a unique characteristic, where each gesture is recorded with a special device designed to capture hand gestures with high precision. The collected data consists of 300 time points with 9 features at each point, resulting in 2700 data points per gesture. Data capture was done at a frequency of 76.92 Hz, where each gesture was recorded with a timestamp every 13 milliseconds, ensuring that each gesture could be analyzed in detail. Each gesture was then saved in a CSV file for easy data management and processing. For each disease class, 20 data were collected, resulting in 100 CSV files covering 5 disease classes: Tonsils, Asthma, Cough, Depression, and Headache. This dataset is expected to provide a strong representation for training machine learning models to recognize gestures accurately so that the developed sign language translator system can work well in various conditions.

2.2.2 Dataset Training Process

The dataset training process is an important stage in building a model using ANN architecture. At this stage, the model is trained using data that has been prepared in order to recognize the patterns and characteristics contained in the dataset. The main objective of this stage is to produce a model that has high generalization ability so that the model can work well on data that has never been seen before.

In testing, the dataset is divided into two parts, namely training data (train) and test data (test), with a ratio of 75:25, where 75% of the data is used to train the model, and the remaining 25% is used to test the performance of the model after training. This division aims to ensure that the model can generalize well and does not experience overfitting of the training data. Testing involves setting several parameters, such as the number of epochs, learning rate, and optimization algorithm, to achieve optimal results. Figure 3 shows the results of the model training process, with an accuracy rate of 100%, indicating that the model could classify each class very well without any identification errors. This accuracy result demonstrates the model's ability to recognize and distinguish gestures in each tested disease class, even on data that has never been processed before. In addition, other evaluation parameters such as F1-score, precision, and recall also reached 100%, which illustrates that the model not only classifies the data correctly (precision) but also has a very high sensitivity in detecting each relevant class (recall). The F1-score reaching 100% indicates a very good balance between precision and recall, which is important to minimize misclassification. These results show that the model has optimal performance in terms of precision and sensitivity to each class-tested. With these excellent results, it can be concluded that the developed model has a very stable and reliable performance in recognizing sign language gestures and is ready to be used in real applications. The model demonstrates outstanding capabilities in gesture recognition and can be relied upon for various applications that require an accurate gesture recognition system.

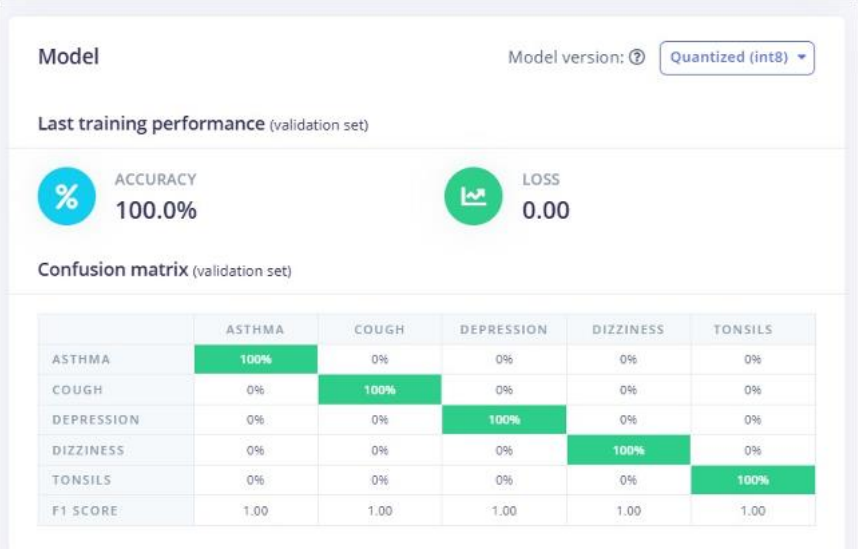

	ASTHMA	COUGH	DEPRESSION	DIZZINESS	TONSILS
ASTHMA	100%	0%	0%	0%	0%
COUGH	0%	100%	0%	0%	0%
DEPRESSION	0%	0%	100%	0%	0%
DIZZINESS	0%	0%	0%	100%	0%
TONSILS	0%	0%	0%	0%	100%
F1 SCORE	1.00	1.00	1.00	1.00	1.00

Figure 3. AI Model Training Result

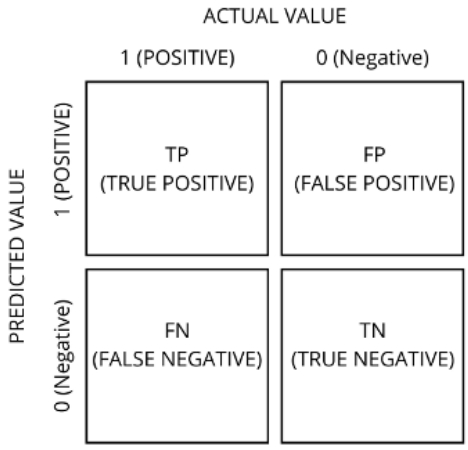

Figure 4. Confusion Matrix Model

2.2.3 Model Performance Measurement

Confusion Matrix is an evaluation method used to measure the accuracy of machine learning model classification results based on the algorithm used. This matrix provides an overview of the model's performance by presenting the number of correct and incorrect predictions. The predicted data is then classified into four main categories, namely positive and negative classes, which include correct predictions for the positive class (true positive), correct predictions for the negative class (true negative), and incorrect predictions for both classes (false positive and false negative).

Figure 4 shows the model prediction results displayed in the form of a Confusion Matrix, which consists of four main categories. First, True Positive (TP) describes the condition where test data that is positive is correctly predicted as positive. Next, False Positive (FP), or Type I error, occurs when data that should be positive is mistakenly predicted as negative. Also, True Negative (TN) is a condition where test data that is actually negative is correctly predicted as negative. Finally, a False Negative (FN), or Type II error, indicates a situation where data that should be negative is wrongly predicted as positive. These four categories help evaluate the accuracy and precision of the

predictions produced by the classification model. From the above, several evaluation metrics can be formulated to measure model performance, such as accuracy, precision, and recall [16].

$$Accuracy = \frac{TP+TN}{TP+FP+TN+FN}\ x\ 100\% \quad (1)$$

$$Precision = \frac{TP}{TP+FP}\ x\ 100\% \quad (2)$$

$$Recall = \frac{TP}{TP+FN}\ x\ 100\% \quad (3)$$

$$F1 - Score = 2\ x\ \frac{Precision\ x\ Recall}{Precision\ +Recall}\ x\ 100\% \quad (4)$$

Confusion matrix is an evaluation tool used to measure the performance of classification models in machine learning by comparing the model's predicted results against the actual labels [17]. The matrix consists of True Positives (TP), True Negatives (TN), False Positives (FP), and False Negatives (FN) elements that facilitate the calculation of various metrics, including accuracy, precision, recall, and F1-score. Accuracy indicates the overall proportion of correct predictions, precision indicates the model'smodel's accuracy in positive predictions, recall measures the model'smodel's ability to recognize positive data, and F1-score balances precision and recall for cases of unbalanced data. The confusion matrix enables comprehensive analysis of model performance, making it an effective tool for assessing the strengths and weaknesses of classification models in each class. The total data used in this research is 100 data for training, 25 data for validation, and 50 data for testing. Sign language recognition in testing is obtained by performing new sign language by disabilities person. The range of accuracy, precision, recall and F1 – Score from 0 -100%. The minimum range of TP, TN, FP, and FN is 0, and the maximum value is 100 in training, 25 data for validation, and 50 for testing.

3. Results

Figure 5 shows the sign language translation device that has been successfully developed in this research. The device is designed to detect and interpret hand and finger movements that represent sign language and translate them into sounds that can be understood by the user. The device consists of several main components, including an EMG sensor to capture hand movements and an MPU6050 sensor to read the angle of hand movements. Further development can be done to improve the translation capabilities, as well as enrich the vocabulary of the signs that can be recognized. The EMG lead in Figure 5 (C) is placed in Flexor Carpi Radialis, Extensor Carpi Radialis, and Brachioradialis muscles.

(**a**) (**b**) **(c)**

Figure 5. Sign Language Interpreting Tool (a) Device Wear by User (b) Whole Device (c) Lead Position in Arm

3.1. Machine Learning Model Accuracy Evaluation

This machine learning model is developed using the ANN algorithm for hand sign language classification. The testing process is conducted through the cross-validation method, which aims to obtain accuracy, precision, recall, and F1-score values that reflect the comprehensive performance of the model. Based on the training results, the model achieved a high accuracy rate of 100% with a low loss value of 0.00%. From the results of the training model obtained, a testing process is carried out using the dataset that was previously taken. The results of testing show that the accuracy value obtained is 96% with a precision value obtained of 97%, which indicates that the model has high accuracy in classifying positive data, while the recall value is 96%, which confirms its ability to detect all positive data. With an F1-score of 96%, the model shows a balance between precision and recall, indicating that the model is consistent and reliable in recognizing hand signals. With this performance, the developed ANN model has a high potential to be used effectively in hand sign language classification applications. The following figure is the result of the model testing that has been done.

The test results in Figure 6 show that the developed artificial intelligence model performed very satisfactorily with a global accuracy rate of 96.00%. Evaluation using confusion matrix revealed that the model was able to classify six categories of health conditions with a high level of precision. From the test results, it was seen that the model achieved 100% perfect accuracy for the categories of tonsils, asthma, depression, and headache, indicating good discrimination ability for these conditions. These results show that the model has great potential in assisting medical diagnosis with a high degree of accuracy.

Further analysis of the F1-Score metric confirmed the consistency of the model's performance, with very high values across all categories tonsils 100%, asthma 89%, cough 100%, depression 100%, and headache 91%. These high F1-Score values indicate an optimal balance between precision and recall, suggesting that the model is not only accurate in its predictions but also consistent in its performance across categories. The only area that requires special attention is the classification of Cough conditions, where the model shows 80% accuracy, with 20% of cases misclassified as tonsillitis. This phenomenon is likely due to the overlap or similarity in symptom manifestation between the two conditions. Nonetheless, an 80% accuracy rate for the Cough category is still a fairly good result in the context of medical classification.

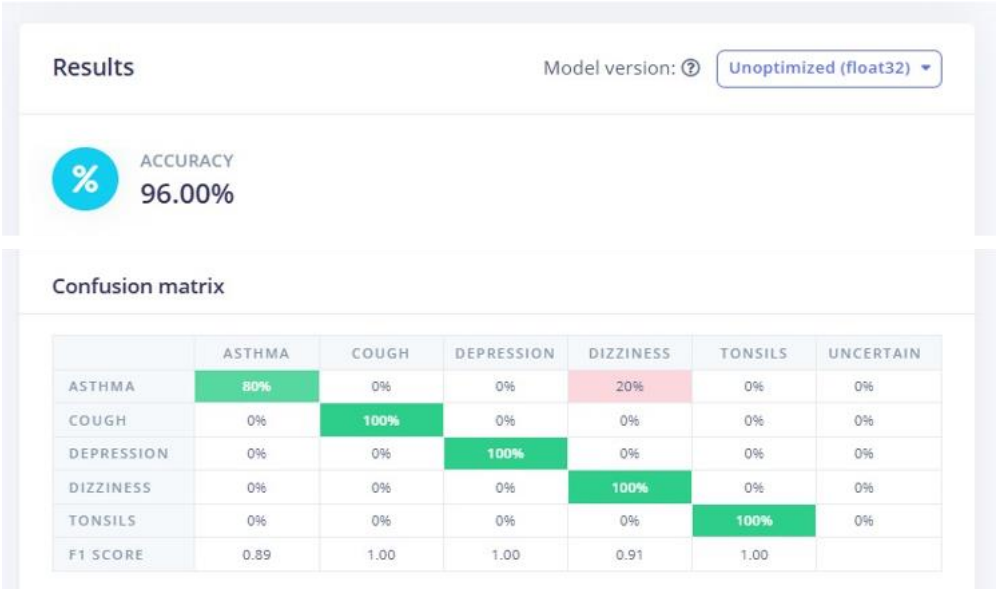

	ASTHMA	COUGH	DEPRESSION	DIZZINESS	TONSILS	UNCERTAIN
ASTHMA	80%	0%	0%	20%	0%	0%
COUGH	0%	100%	0%	0%	0%	0%
DEPRESSION	0%	0%	100%	0%	0%	0%
DIZZINESS	0%	0%	0%	100%	0%	0%
TONSILS	0%	0%	0%	0%	100%	0%
F1 SCORE	0.89	1.00	1.00	0.91	1.00	

Figure 6. Model Testing Results

Based on these test results, it can be concluded that the developed model has significant potential to be implemented in clinical decision support systems. The consistently high performance of the model in almost all categories, as evidenced by the 96.00% global accuracy and excellent F1-Score, indicates the reliability of the model in classifying various health conditions. However, it should be noted that for cases indicated as Cough or Tonsil, additional verification may be required to ensure the accuracy of the diagnosis. This finding also opens up opportunities for further development, particularly in improving the model's ability to distinguish between Cough and Tonsil conditions with more precision.

3.2 Implementation and Test Results of Sign Language Translator System Implementation

The implementation and testing phase of the system was conducted to evaluate the performance of the machine learning-based sign language translator system in identifying hand gestures that represent various types of diseases. The system is focused on five predetermined disease classes, namely tonsils, asthma, cough, depression, and headache. Each disease class is tested ten times to obtain more representative data so that a more accurate picture of the system's performance can be obtained. This test aims to assess the level of accuracy and consistency of the system in recognizing and translating sign language gestures associated with each disease tested. To ensure the objectivity of the results, each experiment was conducted with a wide variety of hand gestures in accordance with sign language standards and was conducted with sufficient repetition to obtain reliable results. The test data obtained is then analyzed to measure how effective this system is in recognizing and classifying hand gestures that represent these diseases. The test results can be seen in more detail in Table 1.

Tests were conducted on five classes of health conditions where Asthma represents Tonsil condition, Cough for Asthma condition, Depression for Cough condition, Dizziness for Depression condition, and Tonsils for Headache condition. Each class underwent ten trials to ensure the consistency and reliability of the model in classifying each of these health conditions. Based on the test results, four out of the five tested classes performed very well, with an accuracy rate of 100%. This perfect accuracy indicates that the system successfully recognized all samples tested in these classes without any errors in the classification process. The success with 100% accuracy in most of these classes confirms that the sign language interpreter system has an excellent ability to distinguish hand gestures representing various diseases and shows high stability and reliability in the classification process despite being tested under uniform and standardized testing conditions.

Table 1. Testing Results of Sign Language Translator System Implementation

	Asthma	Cough	Depression	Dizziness	Tonsils
Asthma	10	0	0	0	0
Cough	0	9	0	0	1
Depression	0	0	10	0	0
Dizziness	0	0	0	10	0
Tonsils	0	0	0	0	10

However, in one of the test classes, the Cough class, there was one misclassification out of five samples tested. This resulted in an accuracy rate for that class of 90%, with an error rate of 10%. This

misclassification could be caused by several factors, including the similarity between the gestures in the class and the gestures from other classes or small variations in the execution of the hand gestures performed by the user during the test. However, even though there was one error in the Asthma class, it did not have a significant impact on the overall performance of the system, as most of the other classes continued to show very high accuracy. Overall, the average accuracy of the system across all classes reached 98%, indicating that the performance of the system in classifying sign language gestures is very good and acceptable.

4. Conclusions

This research successfully developed a machine learning-based sign language translation system using a combination of EMG sensors and MPU6050 on an ESP32 microcontroller. The system can classify five types of gestures representing common diseases with an average accuracy of 98%. The evaluation shows that the system has a high level of precision and recall, which proves the effectiveness of the model in classifying hand gestures with good consistency. The implementation of this system is expected to facilitate communication between people with disabilities and the general public and improve their social inclusion. Further research is recommended to explore the development of the model with a larger number of classes and test the implementation in a real environment to improve the robustness of the system to individual user variations.

References

1. L. Andriyani, "Pemenuhan Hak Disabilitas Perkotaan Dalam Kesetaraan Akses Ekonomi: Pemenuhan Hak Disabilitas Perkotaan Dalam Kesetaraan …," *Sosio Inf. Kaji. Permasalahan Sos. …*, vol. 8, no. 2, pp. 119–130, 2022.
2. R. D. Agustanti, B. Waluyo, and D. A. Ramadhani, "Upaya Peningkatan Pengetahuan Dan Pemahaman Hak-Hak Penyandang Disabilitas Di Bidang Ketenagakerjaan Atas Dasar Persamaan Hak," *JMM (Jurnal Masy. Mandiri)*, vol. 6, no. 5, pp. 3776–3789, 2022, doi: 10.31764/jmm.v6i5.10237.
3. A. Of *et al.*, "Advokasi Pekerjaan Sosial Terhadap Diskriminasi Pada Kaum Penyandang Disabilitas Di Dunia Kerja," *J. Soc. Work Soc. Serv.*, vol. 3, no. 2, pp. 130–138, 2022.
4. A. Nugroho, R. Setiawan, A. Harris, and Beny, "Deteksi Bahasa Isyarat Bisindo Menggunakan Metode Machine Learning," *J. Process.*, vol. 18, no. 2, Nov. 2023, doi: 10.33998/processor.2023.18.2.1380.
5. R. H. Alfikri, M. S. Utomo, H. Februariyanti, and E. Nurwahyudi, "Pembangunan Aplikasi Penerjemah Bahasa Isyarat Dengan Metode Cnn Berbasis Android," *J. Teknoinfo*, vol. 16, no. 2, p. 183, 2022, doi: 10.33365/jti.v16i2.1752.
6. J. Li *et al.*, ""SignRing: Continuous American Sign Language Recognition Using IMU Rings and Virtual IMU Data,"" *Proc. ACM Interactive, Mobile, Wearable Ubiquitous Technol.*, vol. 7, no. 3, pp. 1–29, Sep. 2023, doi: 10.1145/3610881.
7. S. A. Khomami and S. Shamekhi, ""Persian sign language recognition using IMU and surface EMG sensors,"" *Measurement*, vol. 168, p. 108471, Jan. 2021, doi: 10.1016/j.measurement.2020.108471.
8. Y. Gu, C. Zheng, M. Todoh, and F. Zha, ""American Sign Language Translation Using Wearable Inertial and Electromyography Sensors for Tracking Hand Movements and Facial Expressions,"" *Front. Neurosci.*, vol. 16, Jul. 2022, doi: 10.3389/fnins.2022.962141.
9. R. Setiawan, H. H. Triharminto, and M. Fahrurozi, "Gesture Control Menggunakan IMU MPU 6050 Metode Kalman Filter Sebagai Kendali Quadcopter," *Pros. Semin. Nas. Sains Teknol. dan Inov. Indones.*, vol. 3, no. November, pp. 411–422, Dec. 2021, doi: 10.54706/senastindo.v3.2021.133.
10. W. T. Wahyudi, K. Karyanto, and R. M. Antosia, "Rancang Bangun Alat Resistivitas Berbasis Arduino Menggunakan Modul ACS712 dan ADS1115," *J. Tek.*, pp. 1–7, 2021.
11. E. W. Pratama and A. Kiswantono, ""Electrical Analysis Using ESP-32 Module In Realtime,"" *JEECS (Journal Electr. Eng. Comput. Sci.*, vol. 7, no. 2, pp. 1273–1284, 2023, doi: 10.54732/jeecs.v7i2.21.
12. R. Dastres and M. Soori, ""Artificial Neural Network Systems,"" *Int. J. Imaging Robot.*, vol. 21, no. 2, pp. 13–25, 2021.
13. I. Akil, "Komparasi Fungsi Aktivasi Neural Network Pada Data Time Series," *Inti Nusa Mandiri*, vol. 18, no. 1, pp. 78–83, 2023.

14. M. A. Hanin, R. Patmasari, and R. Y. Nur, ""Sistem Klasifikasi Penyakit Kulit Menggunakan Convolutional Neural Network (Cnn) Skin Disease Classification System Using Convolutional Neural Network (Cnn),"" *e-Proceeding Eng.*, vol. 8, no. 1, pp. 273–281, 2021.
15. Alfandi Safira and F. N. Hasan, "Analisis Sentimen Masyarakat Terhadap Paylater Menggunakan Metode Naive Bayes Classifier," *Zo. J. Sist. Inf.*, vol. 5, no. 1, pp. 59–70, 2023, doi: 10.31849/zn.v5i1.12856.
16. Lukman Priyambodo *et al.*, "Klasifikasi Kematangan Tanaman Hidroponik Pakcoy Menggunakan Metode SVM," *J. RESTI (Rekayasa Sist. dan Teknol. Informasi)*, vol. 6, no. 1, pp. 153–160, Feb. 2022, doi: 10.29207/resti.v6i1.3828.
17. A. Ridhovan and A. Suharso, "Penerapan Metode Residual Network (Resnet) Dalam Klasifikasi Penyakit Pada Daun Gandum," *JIPI (Jurnal Ilm. Penelit. dan Pembelajaran Inform.*, vol. 7, no. 1, pp. 58–65, 2022, doi: 10.29100/jipi.v7i1.2410.

COMPLETE
Journal of Computer, Electronic, and Telecommunication
ISSN 2723-4371, E-ISSN 2723-5912

Article

Implementation of IoT Technology in Aquaponics and Modern Aquaculture Systems for Optimizing Catfish Growth

Asep Syaputra[1*], Nanda. S. Prawira[2]

[1,2] Department of Informatics, Institut Teknologi Pagar Alam, Pagar Alam, Indonesia

* Correspondence: asepsyaputra68@itpa.ac.id

Received: 23 November 2024; Revised: 12 December 2024; Accepted: 31 December 2024

Abstract: In the modern era, various systems of agriculture and aquaculture have evolved rapidly. One remarkable innovation is modern aquaponics, a method that is gaining recognition as a sustainable solution for food production. This system combines fish farming and agriculture into a unified and mutually beneficial approach. Modern aquaponics has proven to be effective in overcoming the constraints of urban land, providing a viable solution for both agriculture and aquaculture. For optimal results in fish farming, it is crucial to consistently monitor the conditions of fish growth and health to avoid the risk of crop failure. In response to this challenge, this study aims to implement an Internet of Things (IoT) system in modern aquaponics, focusing primarily on enhancing the growth of catfish in a controlled and efficient manner. This system employs a range of IoT sensors, including pH sensors, Total Dissolved Solids (TDS) sensors, and temperature sensors, to monitor the water quality within the aquaponics setup continuously. Such monitoring not only ensures optimal conditions for healthier fish but also increases plant productivity, thereby enhancing the overall sustainability and effectiveness of the cultivation process. The results of sensor testing revealed a pH value of 7.2, indicating that the water's acidity level is within a balanced and optimal range for supporting the health of catfish. TDS sensor readings showed a value of 300 ppm, suggesting that the concentration of dissolved particles is ideal for the well-being of the fish. Furthermore, temperature measurements from the DS18B20 sensor recorded a water temperature of 28°C, which falls within the optimal range for catfish growth (28–30°C). These conditions create a stable environment that supports the healthy growth of fish in the aquaponics system.

Keywords: Aquaponics, Aquaculture, Catfish Growth Optimization, IoT

1. Introduction

Freshwater fish farming and growth processes typically require substantial space for development. However, the growing demand for food, coupled with limited land availability in urban areas, poses a significant challenge for city dwellers attempting to engage in gardening or fish farming activities. An effective solution to this issue is the adoption of aquaponic systems, which integrate fish farming and plant cultivation into a single, efficient, and eco-friendly system. The aquaponic system operates by utilizing waste products from fish, such as excrement and uneaten feed, as a nutrient source for plants [1]. These nutrients are absorbed by the plants, which simultaneously clean and purify the water before it is recirculated back into the system for reuse by the fish. This process establishes a mutually supportive ecosystem where fish and plants thrive together in a sustainable cycle. One pressing challenge in urban areas is ensuring food security, which aquaponic systems address by enabling sustainable food production within limited spaces [2]. According to the Ministerial Regulation of Marine Affairs and Fisheries of the

Republic of Indonesia Number 17/PERMEN-KP/2020 on the Strategic Plan of the Ministry of Marine Affairs and Fisheries for 2020–2024, the per capita fish consumption target was set at 56.39 kilograms in 2020, rising to 58.08 kilograms in 2021 [3]. This upward trend indicates a growing public awareness of the nutritional benefits of fish as a rich protein source. It also underscores the increasing recognition of fish as a vital component of a healthy and balanced diet for individuals and families alike.

To meet this goal, substantial efforts are necessary to guarantee a sufficient and affordable fish supply for all segments of society, especially in regions lacking direct access to fishing grounds such as oceans or open waters. This limitation highlights the need for reliable and sustainable alternative sources of fish production. One viable solution is the advancement of freshwater fish farming, which can be implemented through traditional pond systems or more innovative methods like aquaponics. Aquaponic systems offer dual benefits: they maximize land-use efficiency and enable the simultaneous cultivation of fish and plants. This integrated approach not only strengthens food security but also improves the availability of locally sourced food in a sustainable and environmentally friendly way.

Catfish is one of the most suitable fish species for cultivation in aquaponic systems due to its ease of production and relatively low cost. It is highly nutritious, offering essential nutrients such as protein, carbohydrates, fats, calcium, phosphorus, and iron, making it a valuable addition to human diets. Because of its significant nutritional benefits, catfish has become a key commodity in national agricultural initiatives [4]. In aquaponic systems, catfish play a vital role in supplying essential nutrients like nitrogen (N) and phosphorus (P) through their waste and uneaten feed. The natural processes within the system rely on beneficial bacteria to convert fish waste and leftover feed into nitrates, which serve as primary nutrients for plant growth. This conversion establishes a symbiotic cycle between fish and plants, ensuring the sustainability of both components in the aquaponic ecosystem while enhancing the overall efficiency of food production [5].

Meanwhile, plants in aquaponic systems play a crucial role in filtering water by removing toxic gases generated as metabolic waste from fish, such as ammonia and carbon dioxide. This filtration process is essential, as the purified water is recirculated back into the system, creating a healthier environment for the fish throughout the cultivation period [6]. During aquaculture, fish produce nitrogen in various forms, including ammonia (NH3-N), nitrite (NO2-N), and nitrate (NO3-N), all of which contribute to the nutrient cycle that supports plant growth. Approximately 80–90% of the ammonia is excreted by fish through osmoregulation, while the remaining 10–20% is released via faeces and urine, which also contain total ammonia nitrogen (TAN). Total ammonia nitrogen consists of two main forms: un-ionized ammonia (NH3), which is toxic at high concentrations, and ionized ammonia (NH4), less harmful to fish. These ammonia compounds are natural byproducts of protein metabolism within the fish, and managing their levels is critical to maintaining a balanced and healthy aquaponic ecosystem. In this system, fish and plants work symbiotically, supporting each other to achieve optimal growth and sustainability [7].

In addition to the challenges posed by limited urban land for catfish farming, farmers encounter several other obstacles in cultivating catfish, whether on a large scale or through aquaponic systems. One of the most significant challenges is the instability of freshwater temperatures, which can inhibit catfish growth. Additionally, maintaining stable levels of Total Dissolved Solids (TDS), water pH, and water turbidity plays a crucial role in determining the growth rate of catfish. These factors are critical as they directly impact the quality of the aquatic environment, which is vital for ensuring fish health and avoiding disruptions that could hinder growth. The three key factors, water pH, TDS levels, and turbidity, significantly influence the quality of the fish's habitat, thereby affecting their health and development [8]. Maintaining optimal water conditions, such as balanced pH, suitable levels of dissolved particles, and adequate water clarity, supports efficient fish metabolism, ultimately enabling their maximum growth potential [9].

To effectively address the issues previously highlighted, adopting innovative and efficient technologies is crucial for comprehensive problem resolution. One promising solution is the

implementation of Internet of Things (IoT) technology, which offers an integrated monitoring and control system to optimize catfish growth in modern aquaponic setups [10]. This IoT system is meticulously designed to enable real-time tracking of environmental parameters through advanced sensors capable of measuring key factors such as water pH, temperature, and density [11]. By continuously monitoring these conditions, IoT technology enables faster, data-driven decisions to maintain optimal water quality and environmental conditions, ultimately improving the efficiency and productivity of the aquaponic system [12].

Every shift in these parameters can be quickly identified, and the gathered data can be monitored live on mobile devices like smartphones, linked directly to a web-based application. This allows fish farmers to supervise more efficiently and take immediate corrective measures if the environmental conditions fall out of line, which ultimately boosts both productivity and the overall health of the fish in the aquaponics system. With this kind of monitoring and control in place, farmers can easily keep track of water quality and act quickly should any abnormalities arise, thus reducing the risk of crop failure. In addition to IoT technology, the system also features a portable function to identify the aquaponics setup location, making it adaptable for both indoor and outdoor placements.

2. Materials and Methods

Research on aquaponics has been conducted by Asep and colleagues in their work titled *"Environmental Management Through Education on Catfish Cultivation Utilizing Aquaponics and Hydroponics as Alternative Solutions for Optimizing Limited Land Use."* This study involved two months of observation with four fish farmers in Pagar Alam City, a region in Indonesia recognized as one of the areas whose primary income is derived from agriculture and tourism. According to Law No. 23 of 1997 concerning Environmental Management, the environment is a unified space that includes all objects and living beings, including humans and their behaviour, which supports the life and well-being of humans and other living creatures. Humans, as the entities with the greatest control over the environment on Earth, play a critical role in maintaining the sustainability of the natural environment [13].

The research findings indicate that the village has significant potential for land utilization in the development of aquaponic systems. Utilizing this land could enhance agricultural and aquaculture productivity in the area. However, to realize this potential fully, it is recommended that the community innovate by adopting more modern hydroponic or aquaponic systems. Such innovations would contribute to improving the local economy and help meet the food demands of Pagar Alam City in the future. Based on the challenges identified, the application of Internet of Things (IoT)-based technology is necessary to address the observed constraints while supporting Indonesia's agenda for the Fourth Industrial Revolution (Industry 4.0). The Minister of Industry, Airlangga Hartarto, has emphasized the importance of digital transformation for Indonesia to remain competitive in the global market, given the rapid advancements in digitalization that now span various industrial sectors.

This study employs the ESP32 and Arduino UNO microcontrollers as the primary control units, integrated with pH sensors, TDS sensors, and DS18B20 temperature sensors to measure water quality parameters. Additionally, the system incorporates several supporting components, including a power supply, step-down module, relay, and aquarium heater.

Figure 1. Arduino UNO

Figure 2. Arduino UNO

As a microcontroller, the Arduino UNO is responsible for transmitting the values obtained from the pH sensor to the ESP32, as illustrated in Figure 1.
As a microcontroller, the ESP32 functions to control various electronic devices and other sensors, as illustrated in Figure 2.

Figure 3. Sensor pH

This sensor functions to measure the acidity or alkalinity of a solution by detecting the concentration of hydrogen ions (H^+) within it. The optimal pH range for catfish habitats is between 6 and 8, as illustrated in Figure 3

Figure 4. DS18B20 Temperature Sensor

This device is used to measure the water temperature in aquaponics systems to enhance the survival and growth of catfish. The measurement is conducted by monitoring the water temperature after it has been filtered through the filter bucket and plant roots. The optimal temperature range for catfish habitats is between 28°C and 35°C, as illustrated in Figure 4.

Figure 5. Sensor TDS

This device is used to measure the concentration of dissolved solids in the water for catfish habitats. The Total Dissolved Solids (TDS) concentration serves as an important indicator of water cleanliness and health. The optimal dissolved solid level for catfish habitats is approximately 300 ppm, as illustrated in Figure 5.

2.1. Research Flowchart

The initial stage of this research involves hardware design, beginning with the development of the Nutrient Film Technique (NFT) module. NFT is a system that utilizes a thin layer of nutrient solution, or 'film,' with a thickness of approximately 1-3 mm. This solution is pumped and continuously circulated over the plant roots at a flow rate of around 1-2 litres per minute. This stable nutrient flow ensures that the plant roots receive an optimal supply of nutrients for growth.

According to S. Wibowo and A. Asriyanti, the steeper the slope of the trough in the NFT system, the higher the plant productivity [14]. This method offers several advantages, including ease of root zone control, ensuring optimal water supply, and the ability to adjust the uniformity and concentration of the nutrient solution based on the plant's age and type. It also offers benefits such as low maintenance costs, better resistance to pests and diseases, and eliminates the need for special fertilization. These advantages make it an efficient solution for plant cultivation systems [15]. Meanwhile, in the aquaculture component, the authors applied the sump filter method to direct water into a bucket tube, replacing the previous chamber setup. After passing through the filtration process in the bucket tube, the filtered water is then pumped back and directed into the aquaponic pipes, ensuring efficient water circulation and maintaining water quality within the system.

2.2. Stages of Equipment Assembly

This graphic representation provides an overview of the workflow and key components in the system design of this study. The diagram illustrates how each part of the system operates and interacts to achieve the goal of monitoring and controlling pH, TDS, and water temperature in the aquaponics system. Figure 2 shows a block diagram outlining the operational mechanism of the device, including how sensors (pH, TDS, and temperature) transmit data to the microcontroller (ESP32 or Arduino UNO), which processes the data and controls devices such as heaters or pumps to maintain optimal water conditions.

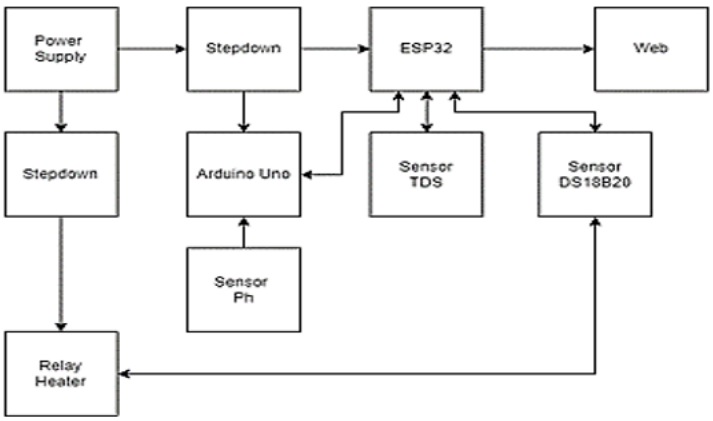

Figure 6. Diagram Blok

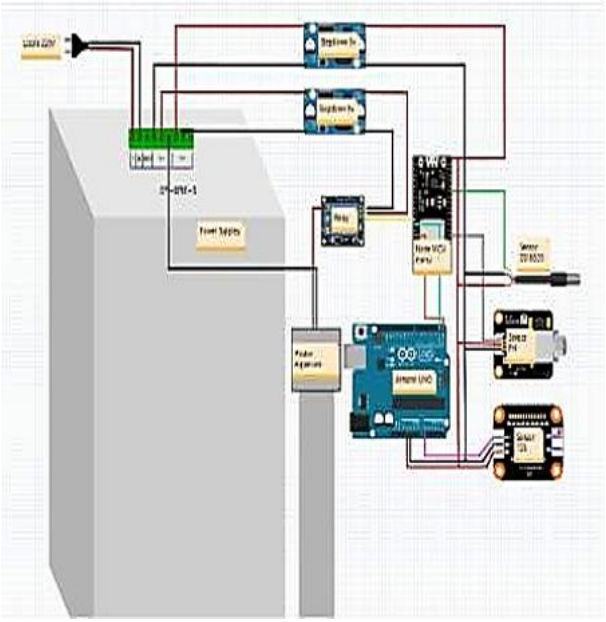

Figure 7. Integration Device Circuit

The schematic diagram of the system can be described as follows:

1. The 12V 20A Power Supply converts AC to DC, providing the necessary power to all components within the system.
2. LM2596 Step-down converter reduces the voltage from 12V to 5V or 3.3V, depending on the requirements of the microcontroller and sensors.
3. NodeMCU ESP32 serves as the primary microcontroller, connecting the system to the Wi-Fi network. It also processes signals from the sensors and transmits data to the user's device via the internet.
4. Arduino UNO receives data from the pH sensor and sends the information in serial data format to the ESP32, enabling the pH values to be displayed on the website.
5. The relay functions as an automatic switch controlled by the microcontroller, allowing the activation or deactivation of devices such as the heater or water pump based on the system's needs.
6. pH Sensor measures the pH level of the water in the catfish aquarium, which is a crucial parameter in maintaining water quality for the health of the fish.
7. TDS Sensor measures the concentration of dissolved solid particles (ppm) in the catfish aquarium water, serving as an important indicator of water quality and health.
8. DS18B20 Sensor monitors the water temperature in the catfish aquarium, as stable and optimal water temperature is essential for the fish's health and comfort.
9. The Aquarium Heater is used to heat the aquarium water, stabilizing the temperature to maintain it within the optimal range for catfish growth.

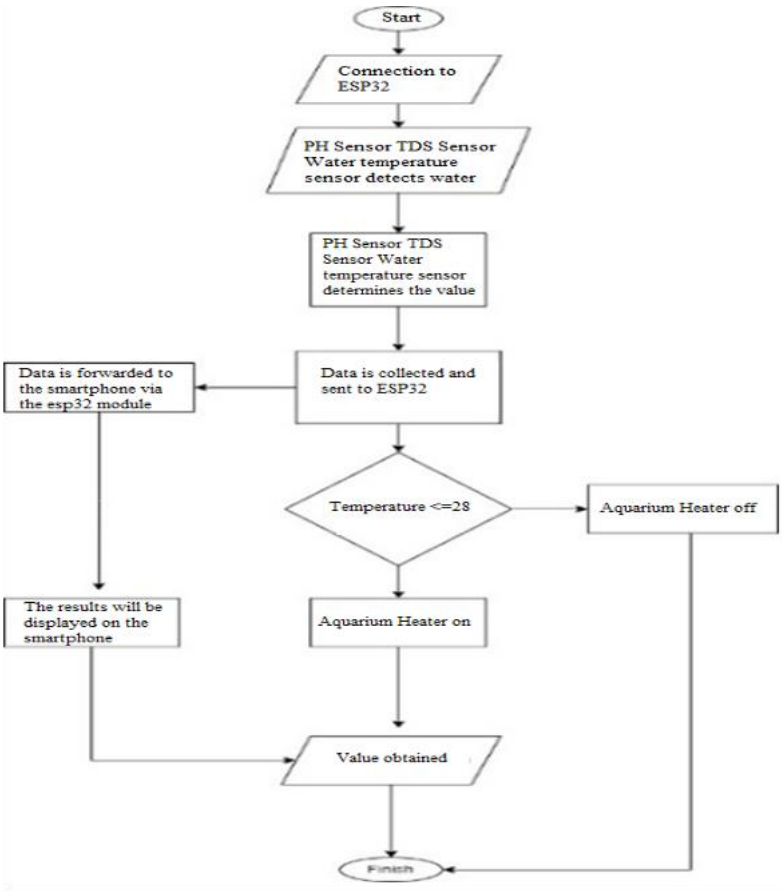

Figure 8. Flowchart of the Process for Displaying Data on the Smartphone

To ensure the clarity and systematic representation of the aquaponics monitoring and control process, a detailed flowchart was developed. The flowchart outlines the sequential flow of activities within the system, starting from data acquisition to controlling specific components based on predefined thresholds. The system begins by initializing the ESP32 and Arduino UNO microcontrollers, which serve as the central control units. Once initialized, the system enters the data acquisition phase, where the pH sensor, TDS sensor, and DS18B20 temperature sensor measure the respective water quality parameters. The microcontrollers then process the collected data, comparing it against preprogrammed threshold values. If any parameter falls outside the acceptable range, the system triggers corrective actions. For instance, when the water temperature drops below the set threshold, the microcontrollers activate the aquarium heater via the relay module. Similarly, the system could send alerts for maintenance if pH or TDS levels deviate significantly. These processes are powered by the LM2596 step-down converter, which ensures a stable voltage supply while the overall power requirement is met by the connected power supply unit.

The integration of Arduino IDE and Fritzing software plays a crucial role in designing the electronic circuit and programming the microcontrollers. The flowchart visually depicts this process, highlighting key decision points and interactions between components, thus enhancing the system's comprehensibility for both developers and researchers. This flowchart-driven approach underscores the efficiency and robustness of the system, aligning with the goals of sustainable aquaponics management. The incorporation of both monitoring and control mechanisms ensures optimal water quality, directly impacting plant and fish health within the aquaponics setup.

3. Results and Analysis

This section presents the results of testing the designed and implemented device, along with an analysis to evaluate the effectiveness of its design and application in a modern aquaponics system

specifically implemented in limited land areas within communities. The implementation of this device aims to address the challenges of urban land constraints, where limited space is a major obstacle in simultaneously cultivating fish and plants. The tests conducted are intended to measure the device's ability to monitor and control key parameters required in the aquaponics system, such as pH, Total Dissolved Solids (TDS), and water temperature. The data obtained from the sensors integrated into the IoT system, which can be monitored in real-time, will be analyzed to assess whether the system can maintain the optimal conditions necessary to support the growth of catfish and plants. Through this analysis, the authors will evaluate the extent to which the device successfully maintains aquaponic environmental quality and provide insights into areas that may require further development to improve system performance and sustainability, particularly in maximizing the potential for agriculture and fish farming in limited spaces.

The pH sensor plays a crucial role in monitoring the environmental conditions within the catfish aquaponics system by ensuring that the water's pH level remains within the optimal range to support the growth and health of both fish and plants. Continuous pH monitoring is essential, as the stability of water quality directly affects the effectiveness and productivity of the overall aquaponics system.

pH sensor testing was conducted over five consecutive days, with data collection once per day, to evaluate the consistency and stability of the pH values within the system's environment. The results of this testing, detailed in Table I, provide insights into the effectiveness of the monitoring process and the potential need for pH adjustments to optimize growth in the aquaponics system.

Figure 9. Implementation of the Device Display

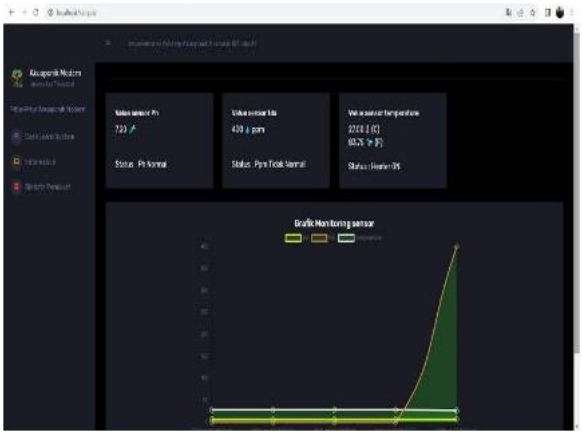

Figure 10. Sensor Data Display on the Web

Table 1. pH Sensor Test Results

Measurement Time	pH Value	Fish Condition	Description
Day -1	7.2	Healthy	pH within the ideal range
Day -2	7.5	Healthy	A slight increase in pH, but it is still within the optimal range
Day -3	7.8	Healthy	The pH continued to increase, requiring immediate action
Day -4	8.1	Fish are stressed	The pH is too high and requires immediate reduction to return to the optimal level
Day -5	7.7	Fish have recovered	The pH has been adjusted back to the optimal range

Table 2. TDS Sensor Test Results

Measurement Time	TDS Value (PPM)	Fish Condition	Description
Day -1	300	Healthy	TDS Value is Vulnerable Within the Optimal Range.
Day -2	350	Healthy	The increase is still within an acceptable range.
Day -3	400	Healthy	The TDS level increased, requiring a reduction to reach the optimal condition.
Day -4	380	Fish are stressed	TDS level decreased and is within a good range.
Day -5	300	Fish have recovered	The TDS level has been adjusted back to the optimal range

TDS sensors play a role in measuring the concentration of dissolved solid particles in the water used for catfish farming, which is an important indicator of water quality in the aquaponics system. Careful monitoring of this parameter is crucial, as optimal water quality directly supports the growth of catfish and maintains their health. The TDS sensor testing was conducted over five consecutive days, with data collection once each day, and the results are presented in Table II. Consistent monitoring is expected to maintain the stability of the aquarium environment and improve the overall productivity of the aquaponics system.

The DS18B20 temperature sensor plays a crucial role in monitoring and controlling the water temperature in the catfish aquaponics system. This sensor works by activating the heater to maintain water temperature stability when it drops below 28°C. Proper and consistent temperature regulation is essential for maintaining the quality of the aquaponics environment, as optimal temperatures support better fish metabolism and plant growth. If the water temperature is too low or high, it can disrupt the health of the fish and plants, as well as reduce the efficiency of the aquaponics system. Therefore, the DS18B20 temperature sensor was tested for five consecutive days to ensure its performance in maintaining the temperature within the appropriate range. Daily recorded temperature data provides valuable information for analyzing the sensor's ability to automatically regulate the water temperature, as shown in the following Table. With effective temperature monitoring, the aquaponics system is expected to operate more optimally, maintaining ideal conditions for the success of both fish farming and crop cultivation in limited spaces.

Table 3. DS18B20 Sensor Test Results

Measurement Time	Water Temperature	Heater Action	Fish Condition	Description
Day -1	28°C	Off	Healthy	The water temperature is within the optimal range without the need for additional heating.
Day -2	25°C	On	Healthy	The water temperature is below the ideal range, so the heater is activated
Day -3	28°C	Off	Healthy	The water temperature has been adjusted back to the optimal range.
Day -4	30°C	Off	Healthy	The water temperature remains stable within the optimal range without the need for heating
Day -5	27°C	On	Healthy	The water temperature did not reach the optimal level, so the heater was activated to stabilize it

4. Conclusion

This study examines the application of Internet of Things (IoT) technology in modern aquaponic cultivation to support the growth of catfish (Oreochromis niloticus) and enhance crop yields. The findings of this research indicate that the application of IoT systems in aquaponics enables real-time, direct monitoring of environmental parameters, including water temperature, total dissolved solids (TDS), and pH levels. With more efficient and accurate monitoring, farmers can take more precise, quick, and appropriate actions in response to changes in environmental conditions. This is crucial to avoid extreme fluctuations that could negatively affect the growth of both fish and plants. Furthermore, the implementation of IoT ensures that environmental parameters remain within the optimal range required by catfish and plants, which in turn has the potential to increase productivity and the quality of aquaponic yields. The study also emphasizes the important role of IoT technology in supporting the sustainability of aquaponic farming. By improving resource efficiency and reducing negative environmental impacts, aquaponics can evolve into a more environmentally friendly system. The application of IoT technology in aquaponics also opens opportunities to integrate other advanced technologies, such as artificial intelligence (AI) and machine learning, which can enhance operational efficiency and productivity in fish and plant cultivation. These technologies enable more accurate and automated decision-making, improve monitoring processes, and optimize environmental conditions to support more optimal growth. Thus, the findings of this study highlight the significant potential of IoT technology in optimizing aquaponic systems, making them a more efficient and sustainable solution in agriculture and aquaculture.

References

1. S. P. Sulaiman, M. S. D. T. S. Arzam, S. P. Ar, M. S. D. A. N. Samsi, And M. S. D. A. Ahmad, Okupasi Lahan Untuk Budidaya Dalam Mendukung Pertanian Berkelanjutan Berbasis Teori Analisis Sistem. Cv. Azka Pustaka, 2024.
2. N. Saskia, D. Firnia, P. Utama, And A. H. Sodiq, "The Efektivitas Rhizobakteria Dan Pupuk Kotoran Kambing Pada Pertumbuhan Dan Hasil Tanaman Bawang Merah (Allium Ascalonicum L.)," Jia (Jurnal Ilm. Agribisnis) J. Agribisnis Dan Ilmu Sos. Ekon. Pertan., Vol. 9, No. 3, Pp. 215–226, 2024.
3. B. Setiawan, S. Styawati, And S. Alim, "Implementasi Sistem Iot Pada Akuakultur Dan Hydroponik (Akuaponik) Modern Untuk Pertumbuhan Ikan Nila," J. Inform. J. Pengemb. It, Vol. 9, No. 1, Pp. 47–53, 2024.

4. M. Handayani, C. Vikasari, And O. Prasadi, "Akuaponik Sebagai Sistem Pemanfaatan Limbah Budidaya Ikan Lele Di Desa Kalijaran," Jtrm (Jurnal Teknol. Dan Rekayasa Manufaktur), Vol. 2, No. 1, Pp. 41–50, 2020.
5. G. M. Samadan, A. Syazili, M. N. Findra, S. Supyan, And Y. D. Wijayanti, "Efektifitas Jenis Tanaman Berbeda Terhadap Kualitas Air Media Budidaya Udang Galah (Macrobranchium Rosenbergii De Man 1879) Sistem Akuaponik," Juv. J. Ilm. Kelaut. Dan Perikan., Vol. 4, No. 1, Pp. 31–42, 2023.
6. N. A. N. Aisyah, A. Sugianti, H. Z. Muhtarom, D. P. Prastyawan, And M. T. Ardiazza, "Implementasi Invoper (Inovasi Pertanian) Dengan Sistem Aquaponik Sebagai Teknologi Tepat Guna Dalam Budidaya Lele," Nusant. J. Pengabdi. Kpd. Masy., Vol. 3, No. 3, Pp. 161–168, 2023.
7. R. A. Nugroho, L. T. Pambudi, D. Chilmawati, And A. H. C. Haditomo, "Aplikasi Teknologi Aquaponic Pada Budidaya Ikan Air Tawar Untuk Optimalisasi Kapasitas Produksi," J. Saintek Perikan., Vol. 8, No. 1, 2012.
8. A. A. E. Astari, K. Merta, N. W. A. Sudiartini, And N. P. P. Sukarini, "Studi Kelayakan Usaha Dan Strategi Pengembangan Budidaya Ikan Lele Di Kota Denpasar (Studi Kasus Petani Ikan Lele Di Ubung Kaja)," J. Jdm, Vol. 4, No. 2, Pp. 108–125, 2021.
9. A. Alwansyah And A. Fahrurozi, "Implementasi Internet Of Thing (Iot) Sistem Monitoring Kualitas Air Shrimp Farming Vaname Pada Aplikasi Berbasis Android," J. Ilm. Teknol. Dan Rekayasa, Vol. 29, No. 1, Pp. 71–85, 2024.
10. N. Fitriana, A. A. Darmawan, And M. F. Rahmawati, "Internet Of Things Untuk Monitoring Kondisi Air Budidaya Ikan Kelompok 'Tutut Jaya'kota Malang," J. Abdimas Nusa Mandiri, Vol. 6, No. 2, Pp. 76–85, 2024.
11. F. P. E. Putra, M. A. Mahmud, And I. S. Maqom, "Pengembangan Sistem Pemantauan Lingkungan Berbasis Internet Of Things (Iot) Di Kampus," Digit. Transform. Technol., Vol. 3, No. 2, Pp. 996–1001, 2023.
12. L. Ihtisyamuddin And M. Mashoedah, "Pengembangan Sistem Monitoring Kualitas Air Dan Pemberi Pakan Otomatis Pada Kolam Budidaya Ikan Lele Berbasis Internet Of Things Di Mbs (Muhammadiyah Boarding School) Yogyakarta," J. Electron. Educ., 2023.
13. P. R. Indonesia And W. Nusantara, "Undang Undang No. 23 Tahun 1997 Tentang: Pengelolaan Lingkungan Hidup," Lembar Negara Ri Tahun,(3699), 1997.
14. P. Puspitahati, R. Andini, And H. P. Rahmad, "Urban Farming Dengan Sistem Hidroponik Nft (Nutrient Film Technique) Dipengaruhi Kemiringan Talang Dan Debit Air Pada Produksi Tanaman Pakcoy (Brassica Rapa Chinensis)," In Seminar Nasional Lahan Suboptimal, 2021, Pp. 835–843.
15. Q. A'yunin Et Al., Perikanan Berkelanjutan. Universitas Brawijaya Press, 2021.

COMPLETE
Journal of Computer, Electronic, and Telecommunication
ISSN 2723-4371, E-ISSN 2723-5912

Article

Design of Micro Wind Power Plant using Dual Savonius Turbines

Risna Risna[1], Riza Hadi Saputra[2*], Fitri Oktafiani[3], Yusuf Cahyo Sampurno[4], Jheskia Ardito[5]

[1, 3, 4] STT Migas Balikpapan, Balikpapan, Indonesia
[2, 5] Institut Teknologi Kalimantan, Balikpapan, Indonesia

* Correspondence: riza.saputra@lecturer.itk.ac.id

Received: 11 October 2024; Revised: 3 December 2024; Accepted: 31 December 2024

Abstract: Wind power plants are one of the renewable energy solutions that are environmentally friendly and sustainable. The success of such plants heavily depends on the location, which plays a crucial role in determining the availability of wind. In addition to highlands, coastal areas can serve as suitable locations. Balikpapan, with its expansive coastlines, holds significant potential for harnessing wind energy as a source of electricity. However, the utilization of this wind energy, particularly on a micro-scale, remains suboptimal. Research conducted over three days recorded wind speeds between 4 m/s and 5 m/s, generating voltages between 3 volts and 4 volts, which is only 1/3 of the total potential voltage. There is still an untapped potential of about 2/3 or 6 volts that could be harnessed if wind speeds reach 12 m/s to 15 m/s. The study concludes that the wind speed at Airport Beach is not yet sufficient to produce the maximum possible voltage. The current wind speeds are only capable of powering a 5-volt capacity light, with the generated energy stored in a battery for later use.

Keywords: Coastal Areas, Renewable Energy, Voltage, Wind Power Plant, Wind Speed

1. Introduction

In support of global efforts toward sustainable energy and the green energy transition, Wind Power Plants are increasingly recognized as one of the most environmentally friendly renewable energy solutions [1]. Wind power plants utilize the kinetic energy of wind to generate electricity, offering a viable alternative that does not produce greenhouse gas emissions during operation. The success of Wind power plant development is largely contingent upon the careful selection of suitable locations where wind speed and patterns are adequate to ensure optimal electricity generation efficiency [2]. While highland regions are often preferred for wind power plant installations due to stronger wind currents, coastal areas also present significant potential, particularly in tropical countries like Indonesia, where coastal winds are generally more stable and consistent. The combination of suitable wind patterns, sustainable energy policies, and advancements in wind turbine technology has the potential to accelerate the deployment of wind power plants in these regions, contributing significantly to national energy security and the global push for low-carbon energy systems [3].

Balikpapan, located on the eastern coast of Kalimantan Island, boasts expansive coastlines and stable wind conditions throughout the year, making it an ideal location for developing wind power plants. Despite its potential, the wind energy resources in this area have not been fully exploited, particularly at the micro-scale level, which would be well-suited to meet local energy needs. Micro-scale wind power plants offer a flexible and scalable approach to harnessing renewable energy, providing a decentralized energy solution that can reduce reliance on traditional fossil fuels and

contribute to local sustainability efforts. In this context, research focused on the design and implementation of micro-scale wind power plants is becoming increasingly critical, particularly in light of the growing demand for green energy [4]. This aligns with the strategic plans for the new capital city, Ibu Kota Negara (IKN) Nusantara, also located in East Kalimantan. As a future-oriented city, IKN aims to prioritize the use of renewable energy as part of its smart and sustainable city vision [5]. The development of renewable energy infrastructure, such as micro-scale wind power plants, could play a pivotal role in realizing this vision, supporting both regional and national goals for energy transition and environmental sustainability [6].

This research focuses on the innovative design of a micro-scale wind power plant utilizing dual Savonius turbines optimized for the wind conditions along the coast of Balikpapan. The Savonius turbine was chosen due to its ability to operate efficiently at low wind speeds, which are commonly found in coastal areas. Although the Savonius turbine generally has lower efficiency compared to conventional lift-type wind turbines, its advantage lies in its ability to initiate operation at slow wind speeds, offering significant opportunities for further optimization through advanced design improvements [7]. One of the key strategies proposed in this study is the implementation of a dual turbine configuration to enhance wind capture capacity and improve energy conversion efficiency [8]. Positioning two Savonius turbines in tandem or side-by-side is expected to increase the effective surface area exposed to the wind, thereby improving power output. Additionally, the study explores the potential for optimizing the rotor shape, blade curvature, and turbine spacing to maximize performance under varying wind conditions, contributing to more reliable and sustainable energy generation for local coastal communities [9].

The development of this micro-scale wind power plant will be carried out in a phased approach over a five-year period. In the first year, the focus will be on the initial design and simulation of the dual Savonius turbine system [10]. This stage will involve creating a conceptual model and conducting simulations to predict the turbine's performance under specific wind conditions in coastal Balikpapan [11]. The second year will be dedicated to design optimization, where key parameters such as blade size, angle of attack, and overall turbine geometry will be refined based on the results of the initial simulations [12]. The goal will be to maximize efficiency and adapt the turbine to the low wind speeds typical of coastal environments. In the third year, a prototype will be built, and initial field testing will be conducted to assess real-world performance and collect operational data. This data will be used to identify any necessary adjustments and to validate the simulation models [13]. The fourth year will see the final design phase, where efforts will be focused on minimizing energy losses and enhancing power output through advanced engineering solutions. Finally, in the fifth year, the micro-scale wind power plant will be implemented at a selected coastal site in Balikpapan, followed by extensive field evaluations to monitor system performance under actual operational conditions. This step will provide valuable insights into the practical feasibility and sustainability of the system, guiding future deployments and improvements [14].

In relation to IKN, the outcomes of this research are expected not only to provide a renewable energy solution for the local community in Balikpapan but also to contribute to the vision of IKN as a self-sustaining green city. Given the geographic proximity between Balikpapan and the IKN Nusantara site, the successful implementation of an efficient micro-scale wind power plant along the coast of Balikpapan could serve as a model for further development in the IKN area. Harnessing wind energy as part of the renewable energy portfolio for the new capital city would align with its goals of reducing reliance on fossil fuels and achieving long-term sustainability [15]. The deployment of such technology could complement other renewable energy sources, such as solar and hydropower, providing a diversified and resilient energy infrastructure for IKN [16]. Furthermore, this research holds strategic importance beyond local implementation, as it supports national green energy initiatives, particularly in East Kalimantan, where transitioning to renewable energy sources is critical for the region's economic and environmental future. By integrating micro-scale wind power plants into the broader energy strategy of IKN, this project could become a pivotal element in advancing Indonesia's commitment to reducing greenhouse gas emissions and promoting sustainable urban development.

2. Materials and Methods

The approach used in this research involves a research and development process focused on the Savonius turbine. This means that the turbine design will be optimized based on previous research findings as well as new insights gained during the research and development process. The goal is to create a turbine design that can significantly improve the efficiency of electricity generation, thereby making the micro-scale wind power plant a viable and sustainable renewable energy solution. This iterative research and development process will incorporate advanced computational simulations, material selection, and aerodynamic analysis to refine the turbine's performance, particularly in low-wind-speed environments typical of coastal areas. By integrating the latest technological innovations and addressing challenges such as reducing drag and enhancing rotational efficiency, the project aims to develop a more robust and scalable turbine design. Ultimately, this research seeks to contribute to the global effort to increase the adoption of renewable energy technologies by providing a practical and efficient solution that can be implemented in similar coastal regions with comparable wind conditions.

The Savonius turbine, a type of drag-based wind turbine, has the advantage of being able to start operating at low wind speeds. However, its efficiency is relatively lower compared to lift-based wind turbines. Several studies have been conducted to improve the efficiency of the Savonius turbine, yet its application at the micro-scale, particularly in Indonesia, remains rare. This research aims to develop, design, and implement a micro-scale wind power plant featuring dual Savonius turbines optimized for the specific wind conditions found along the coast of Balikpapan. The dual-turbine configuration is expected to enhance wind capture and improve overall energy conversion efficiency by increasing the swept area and optimizing the arrangement of the turbines. The research will also explore innovative modifications to turbine geometry, such as blade shape and spacing, to maximize performance under low and variable wind speeds. The outcomes of this study have the potential to provide a renewable energy solution for the surrounding community, offering a sustainable and scalable model for coastal regions with similar wind profiles. This project not only contributes to the body of knowledge on micro-scale wind energy systems but also supports local and national goals for increasing the use of clean energy sources.

The research roadmap focuses on the design and development of a micro-scale wind power plant utilizing dual Savonius turbines along the coast of Balikpapan. In the first year, the project will concentrate on the initial design and simulation of the turbine system, using computational tools to model performance under the specific wind conditions of the area. The second year will focus on optimizing the turbine design and constructing a working prototype, with adjustments made to key parameters such as blade geometry, rotor configuration, and material selection. In the third year, the prototype will undergo field testing, and data will be collected to analyze its operational performance in real-world conditions. Based on the testing results, design refinements will be made in the fourth year, culminating in the construction of the final version of the micro-scale wind power plant. In the fifth and final year, the optimized wind power plant will be implemented at a selected coastal site, followed by comprehensive field evaluations to assess its long-term performance and viability as a renewable energy solution. This research is expected to provide a sustainable energy alternative for the local community, helping to reduce reliance on non-renewable energy sources and contributing to broader national goals for renewable energy adoption. Figure 1 presents the research roadmap in detail.

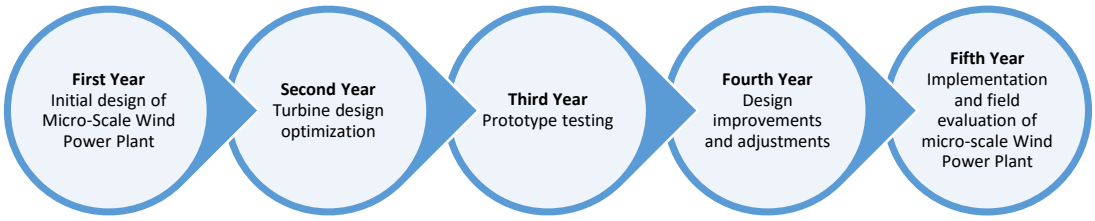

Figure 1. Research Roadmap

The research process begins with a comprehensive review of relevant literature, which is a critical foundation for the success of the study. This literature review includes an analysis of previous studies on Savonius turbines and wind power plants that have been developed and tested by other researchers. The review not only identifies gaps in the existing research but also highlights key findings that can inform the current project. By thoroughly understanding the performance characteristics, efficiency challenges, and design innovations from earlier work, the researchers can develop a solid framework for their own study. This foundational knowledge provides insights into various design strategies, material choices, and technological advancements that can be leveraged for the construction of a more efficient dual Savonius turbine system. The next step after completing the literature review is the detailed design of the dual Savonius turbine, tailored to the specific wind conditions at the coastal site in Balikpapan. Factors such as wind speed, turbulence, and directionality are taken into account to optimize the turbine's design. The goal is to maximize the efficiency of power generation, even at low wind speeds, by considering the ideal blade shape, turbine size, and overall system configuration. Once the design is finalized, the team proceeds with constructing the prototype of the micro-scale wind power plant.

The construction phase involves integrating various materials and components, including control equipment such as an Arduino Leonardo for real-time monitoring and control, a sturdy frame to support the dual Savonius turbines, and essential sensors to measure wind speed and voltage output. Additionally, an anemometer is used to measure and calibrate wind speed data, ensuring that the system is accurately adjusted to the local environmental conditions. The physical assembly of the turbines and the associated electrical system is a crucial stage, as it directly impacts the plant's performance. Once the wind power plant prototype is built, the system is tested at a selected coastal site in Balikpapan to assess its real-world performance. This testing phase aims to verify the operational efficiency of the turbines and evaluate their ability to generate usable electricity for the local coastal community. During testing, key data such as voltage, current, and overall power output are meticulously collected. The data is essential for a detailed analysis of the wind power plant's performance, helping to identify any areas for optimization or further development. After the field tests, the collected data is analyzed to assess the efficiency, reliability, and potential improvements for the system. Based on this analysis, the researchers draw conclusions regarding the viability of the design and its implications for renewable energy deployment in coastal areas and offer recommendations for future studies. These conclusions could include suggestions for refining the turbine design, improving system durability, and scaling up the technology for larger applications. Figure 2 illustrates the detailed flowchart of the entire research process.

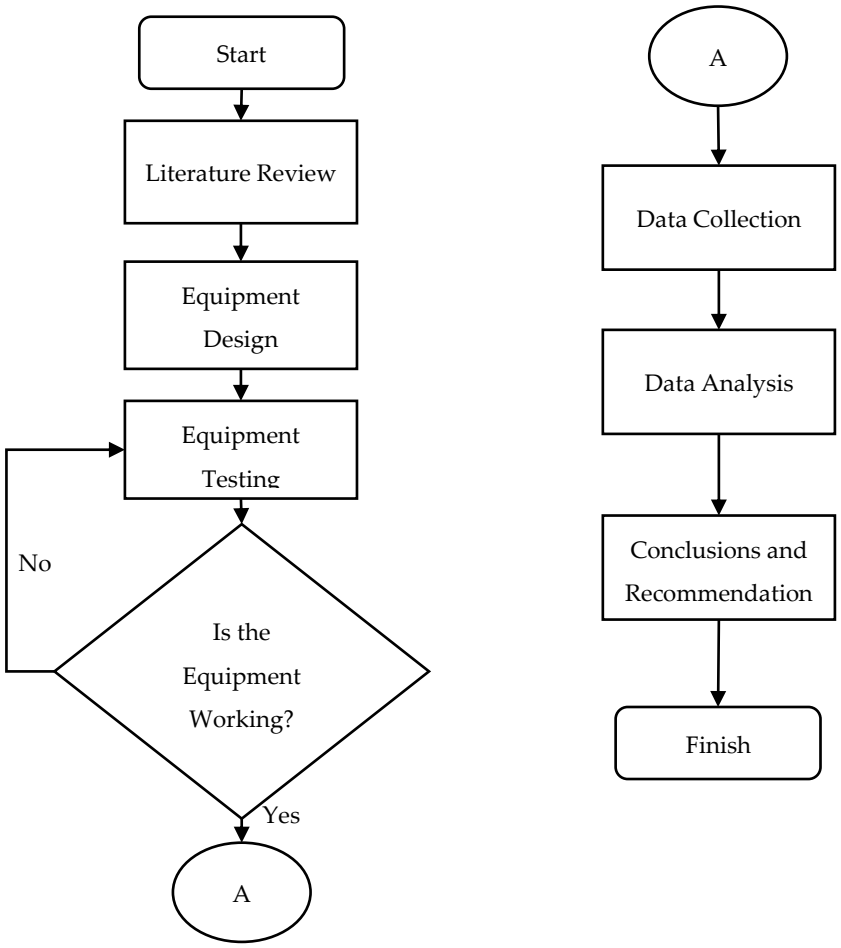

Figure 2. Flowchart Research

3. Results

The research was conducted over three days at Airport Beach, Gunung Bahagia, South Balikpapan, East Kalimantan. Data collection was carried out for one hour each day, specifically between 09:00 and 10:00 WITA (Central Indonesian Time). This time window was likely chosen to capture consistent wind patterns during morning hours when coastal winds are typically more stable. The experiment aimed to gather crucial data on wind speed and the electrical output of the wind turbine system that had been designed and constructed for this research. The equipment used for the data collection included a dual Savonius turbine, an anemometer to measure wind speed, a voltage sensor, and a data-logging system connected to a laptop for real-time monitoring and analysis. The setup was designed to assess the performance of the micro-scale wind power plant (PLTB) under the natural wind conditions found at the coastal location.

The analysis of the wind turbine system depicted in Figure 3 focuses on its potential to generate electrical energy through wind-driven mechanical motion. With a blade diameter of 100mm and a vertical-axis design, the turbine is optimized for omnidirectional wind capture. The motor, with a rated speed of 100 to 6000 rpm, can produce an output voltage ranging from 0.01V to 5.5V and a current of 0.01 to 100mA, depending on the wind speed and rotational velocity of the blades. At low wind speeds (<5 m/s), the output voltage is minimal due to insufficient torque; however, moderate to high wind speeds (>5 m/s) enable the system to reach higher voltages and current outputs, approaching the motor's rated maximums.

The dual vertical-axis wind turbine system, as depicted, consists of two turbines mounted symmetrically on a Y-shaped structure with a central pole height of 200 cm and a horizontal span of 150 cm, providing adequate spacing to minimize aerodynamic interference. The vertical-axis design allows the turbines to capture wind from any direction, making them suitable for variable wind

conditions, while the separation between the turbines reduces wake effects and enhances efficiency. The structure's elevation ensures exposure to stronger wind currents, although it must be robust enough to withstand mechanical stresses from simultaneous wind forces on both turbines. Each turbine independently generates a voltage range of 0.01V to 5.5V (0.02V – 11.0V for both turbines), with the potential for combined output depending on the electrical configuration, doubling the energy capture without a significant increase in structural footprint.

Figure 4 provides a detailed view of a wind energy experiment being conducted at a beach, likely as part of a project to test the performance of micro-scale wind turbines. The first segment of the figure (left) shows a researcher holding an anemometer, a handheld device used to measure wind speed and temperature. The display indicates a wind speed of 3.7 meters per second and a temperature of 29.1°C, offering crucial data about the environmental conditions in which the experiment is taking place. In the background, a laptop is set up on a wooden table, likely being used to log data or monitor the turbine's performance. The beach setting, with the ocean in the distance, provides a natural environment for testing wind energy solutions, taking advantage of the steady coastal winds.

In Figure 4, in the second segment (middle), two individuals are seen assembling or adjusting the wind turbine system, which appears to feature a dual Savonius turbine design. The Savonius turbine is often chosen for low wind speed environments like coastal regions due to its ability to start operating in lower wind conditions. The individuals are working on a horizontal frame, attaching two turbines at either end of the structure. This suggests that they are refining the design to optimize the turbine's wind capture capabilities. The table is cluttered with tools and materials, indicating that they are still in the process of adjusting the equipment for field testing. The surrounding environment, including the tree and beach, indicates that the experiment is being conducted in an open outdoor setting where natural wind conditions can be measured and utilized.

In Figure 4, the third segment (right) shows the completed experimental setup, with the dual Savonius turbines now fully assembled and anchored into place on the beach. A laptop remains connected to the system, likely collecting data such as voltage output and wind speed to analyze the turbine's efficiency. The position of the equipment near the shoreline suggests that the experiment is designed to test the performance of the wind turbines under real-world coastal wind conditions, which tend to vary in speed and direction. This setup appears to be part of a broader research effort to develop a micro-scale wind power plant that can be implemented in coastal regions like Balikpapan. The purpose of this field test is likely to evaluate how well the turbine system generates electricity in low to moderate wind conditions, with the goal of improving renewable energy solutions for local communities.

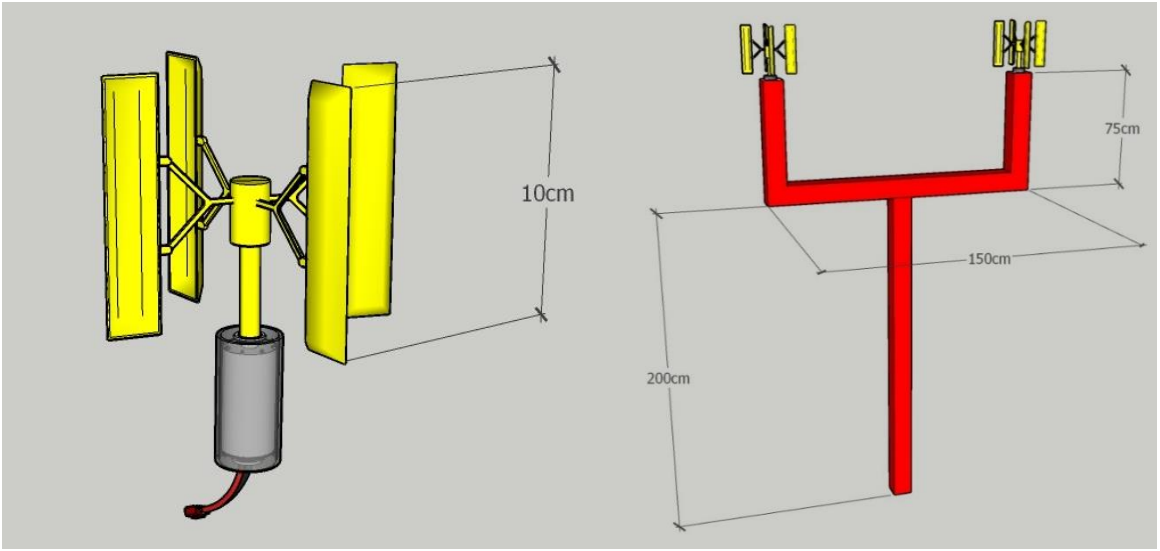

Figure 3. Wind Turbine Design

Figure 4. Field Experiment

Table 1. Spesification of Generator

Specifications	Value
Motor Type	DC (Generator)
Generator Voltage	DC 0.01V - 5.5 V
Generator Current	0.01 - 100mA
Sum of Propeller	4 Propeller
Speed of Propeller	10.5 – 628.3 m/s

Table 1 provides detailed information about the key parameters of the generator used in the research setup. The generator is of the DC (Direct Current) type, commonly employed in small-scale wind turbine systems due to its ability to convert mechanical energy (from the propeller) into electrical energy.

The generator voltage range is specified as 0.01V to 5.5V, indicating that the generator can operate within this voltage range depending on the wind speed and the rotational speed of the propeller. Similarly, the generator current is stated as 0.01mA to 100mA, signifying the range of current output the generator can produce, likely varying with wind conditions and turbine efficiency.

The generator is equipped with four propellers designed to capture the wind and convert kinetic energy into mechanical rotation. The speed of the propeller is specified as ranging from 10.5 m/s to 628.3 m/s, which reflects the range of rotational speeds the propellers can achieve under different wind conditions. The higher end of this range suggests that the system is capable of operating at relatively high wind speeds, contributing to the potential for higher power output.

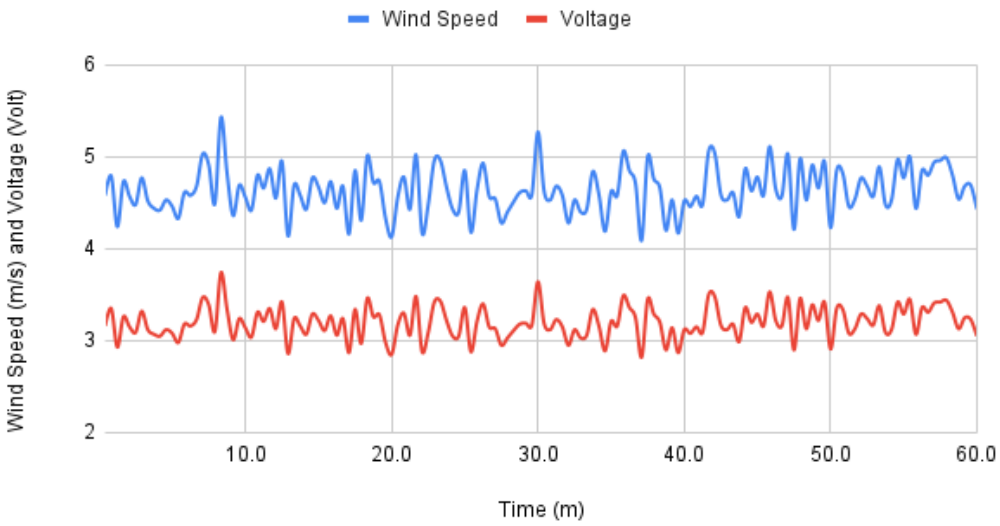

Figure 5. Wind Speed Vs Voltage for Day 1

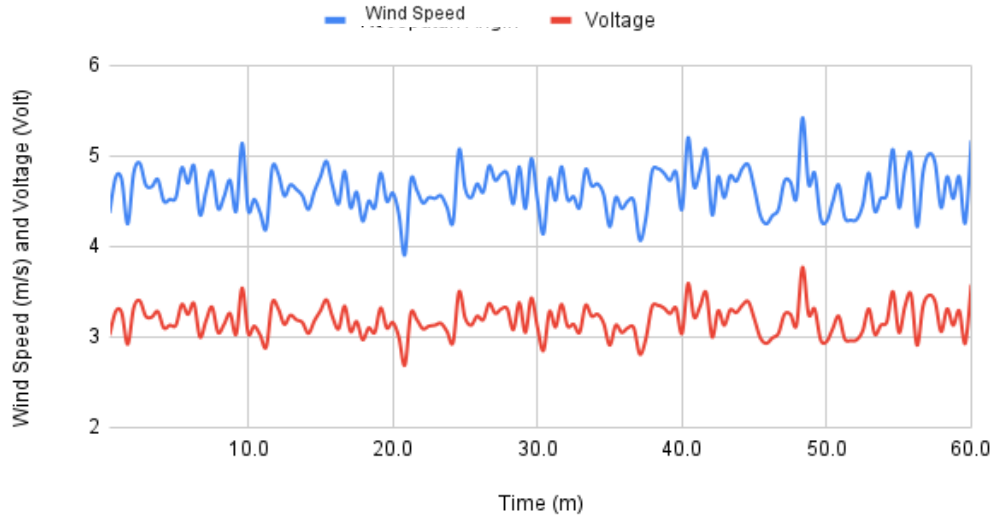

Figure 6. Wind Speed Vs Voltage for Day 2

Figure 5 illustrates the relationship between wind speed (m/s) and voltage (V) generated over a period of time on Day 1 of the experiment. The x-axis represents time in minutes, ranging from 0 to 60, while the y-axis shows both wind speed in meters per second (m/s) and voltage in volts (V). Two lines are plotted: a blue line representing wind speed and a red line representing the voltage output of the generator. The wind speed (blue line) fluctuates consistently throughout the duration of the experiment, generally ranging between 4 m/s and 5 m/s, with occasional spikes above 5 m/s. These variations in wind speed reflect the natural variability of coastal wind conditions, where brief increases and decreases in wind intensity occur frequently. Correspondingly, the voltage output (red line) follows a similar pattern but at a lower magnitude. The voltage fluctuates around 3 V to 3.5 V, with small peaks aligning with increases in wind speed. The voltage curve exhibits smaller variations compared to wind speed, indicating that while wind speed directly impacts voltage generation, the generator maintains a relatively steady output.

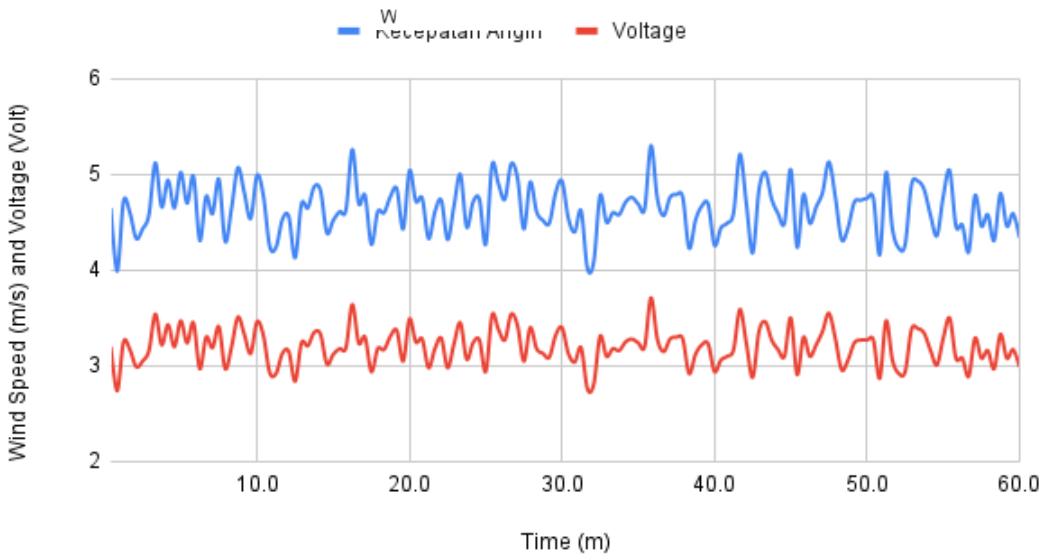

Figure 7. Wind Speed Vs Voltage for Day 3

Figure 6 presents the relationship between wind speed and voltage generated on Day 2 of the experiment, measured over a 60-minute period. The x-axis represents time in minutes, ranging from 0 to 60, while the y-axis shows both wind speed in meters per second (m/s) and voltage in volts (V). The blue line represents wind speed, while the red line represents the voltage produced by the generator. On Day 2, the wind speed fluctuates consistently, primarily within the range of 4 m/s to 5 m/s, with occasional peaks slightly above 5 m/s, similar to Day 1's data. The fluctuations in wind speed are relatively stable, though there are minor spikes, especially towards the later minutes of the experiment. The voltage output, represented by the red line, varies within a narrow range, mostly between 3 V and 3.5 V. Like the previous day, the voltage follows the wind speed fluctuations but maintains a lower, more stable trend. The voltage curve shows smaller variations compared to wind speed, indicating that while wind speed impacts the voltage generation, the system provides consistent electrical output despite the variability in the wind.

Figure 7 illustrates the relationship between wind speed and voltage on Day 3 of the experiment. The x-axis represents time in minutes over a 60-minute period, while the y-axis displays wind speed in meters per second (m/s) and voltage in volts (V). The blue line represents wind speed, and the red line represents the voltage output. On Day 3, the wind speed fluctuates within a range of 4 m/s to 5 m/s, showing a similar pattern to Days 1 and 2. The wind speed demonstrates consistent oscillations with some moderate peaks, especially around the 10, 30, and 50-minute marks. These fluctuations in wind speed are natural, reflecting typical coastal wind variability. The voltage output, on the other hand, remains relatively steady, fluctuating between 3 V and 3.5 V, mirroring the wind speed pattern but with less pronounced peaks. The voltage output appears stable with small variations, indicating that the wind turbine system is converting wind energy into electrical energy consistently despite the variability in wind speed.

4. Discussion

The detailed analysis of the wind speed and voltage output data from Day 1, Day 2, and Day 3 provides insights into the performance and limitations of the micro-scale wind power system. Over the three days, wind speeds fluctuated between 4 m/s and 5 m/s, with some occasional spikes exceeding 5 m/s. These speeds, while steady and consistent for a coastal environment, are moderate and do not reach the higher velocities needed for maximizing the voltage output. The wind turbine system, equipped with dual Savonius turbines, responded predictably to these variations, producing voltage outputs that remained relatively stable within the range of 3 V to 3.5 V. The data shows that

the system functions reliably in low to moderate wind speeds, but there are limitations in the amount of power that can be generated under these conditions.

Throughout the three days, the voltage output closely followed the wind speed fluctuations. Higher wind speeds resulted in slight increases in voltage, but the system's overall output remained within a moderate range. This stable performance is indicative of the Savonius turbine's strength in maintaining a consistent output in low-wind-speed environments, where more conventional turbines might struggle to generate power. However, the voltage generated over the three days was not sufficient to power complex systems or higher-capacity devices. The turbine system produced enough voltage to power devices requiring low energy consumption, such as small lights or other low-power electronics.

The results of the study indicate that the wind speeds at Bandara Beach are not sufficient to generate the maximum possible voltage. The current wind speeds are only capable of producing enough power to operate a 5-volt capacity light, with the excess energy stored in a battery for later use. This highlights the need for additional wind turbines or more efficient turbine designs to increase the voltage output. By incorporating additional turbines or optimizing the current system, it may be possible to achieve higher voltage levels, which could then be used for more complex energy needs, such as powering larger devices or contributing to local energy grids. The findings suggest that while the current system is effective for small-scale energy needs, further enhancements are necessary to fully realize its potential in more demanding applications.

5. Conclusions

The data collected over the course of three days showed that wind speeds at Bandara Beach consistently ranged between 4 m/s and 5 m/s, resulting in a voltage output of 3 V to 4 V. This output represents only about one-third of the total potential voltage that could be generated. There remains untapped potential for an additional two-thirds of the voltage, or approximately 6 volts, which could be harnessed if wind speeds were higher, around 12 m/s to 15 m/s. The findings indicate that the wind speeds at Bandara Beach were insufficient to generate the maximum possible voltage, limiting the turbine system's ability to produce energy beyond powering a 5-volt capacity light, with the excess energy stored in a battery for later use. These results underscore the fact that the system is not fully optimized for more complex energy demands under the current wind conditions. To increase voltage output and meet more substantial energy needs, it is necessary to incorporate additional wind turbines or further refine the existing turbine design. This would allow the system to reach higher voltage levels and be applied in more complex settings, such as powering larger devices or contributing to local energy grids. Additionally, future research should explore the feasibility of testing the turbine system in locations with higher wind speeds, such as mountainous regions or other coastal areas, to evaluate the system's full potential under varying environmental conditions. By expanding the research to other locations, it may be possible to achieve higher wind speeds and, consequently, greater energy generation efficiency.

References

1. R. Gianto, “Model Rangkaian-T Pembangkit Listrik Tenaga Bayu untuk Analisis Aliran Daya Tiga-Fase,” *J. Nas. Tek. Elektro dan Teknol. Inf.*, vol. 10, no. 1, pp. 91–99, 2021, doi: 10.22146/jnteti.v10i1.902.
2. D. Irwansyah *et al.*, “Konversi Energi Listrik Pada Pembangkit Listrik Tenaga Surya dan Pembangkit Listrik Tenaga Bayu Sebagai Perencanaan Pembangkit Hybrid,” *Pros. - Semin. Nas. Tek. Elektro UIN Sunan Gunung Djati Bandung*, pp. 113–127, 2021, Accessed: Oct. 11, 2024. [Online]. Available: https://senter.ee.uinsgd.ac.id/repositori/index.php/prosiding/article/view/senter2020p13
3. D. N. Anwar, Sulaeman Deni Ramdani, Moh Fawaid, Hamid Abdillah, and Muhammad Nurtanto, "PENGEMBANGAN PEMBANGKIT LISTRIK TENAGA BAYU TIPE HAWT 3 PROPELER SEBAGAI MEDIA PEMBELAJARAN: KONSEPTUAL KONVERSI ENERGI," *Steam Eng.*, vol. 2, no. 2, pp. 65–72, 2021, doi: 10.37304/jptm.v2i2.2417.

4. S. Chegini, M. Asadbeigi, F. Ghafoorian, and M. Mehrpooya, "An investigation into the self-starting of darrieus-savonius hybrid wind turbine and performance enhancement through innovative deflectors: A CFD approach," *Ocean Eng.*, vol. 287, Nov. 2023, doi: 10.1016/j.oceaneng.2023.115910.
5. R. N. Jarudkar and Y. P. Deshmukh, "Measurement and analysis for the improvement of efficiency and power of Savonius vertical axis wind turbines without dimples and fins," *Mater. Today Proc.*, vol. 62, pp. 2016–2020, 2022, doi: 10.1016/j.matpr.2022.02.294.
6. M. Badrul Salleh, N. M. Kamaruddin, P. How Tion, and Z. Mohamed-Kassim, "Comparison of the power performance of a conventional Savonius turbine with various deflector configurations in wind and water," *Energy Convers. Manag.*, vol. 247, 2021, doi: 10.1016/j.enconman.2021.114726.
7. Y. Chen, P. Guo, D. Zhang, K. Chai, C. Zhao, and J. Li, "Power improvement of a cluster of three Savonius wind turbines using the variable-speed control method," *Renew. Energy*, vol. 193, pp. 832–842, Jun. 2022, doi: 10.1016/j.renene.2022.05.062.
8. M. Ali *et al.*, "Low profile wind savonius turbine triboelectric nanogenerator for powering small electronics," *Sensors Actuators A Phys.*, vol. 363, 2023, doi: 10.1016/j.sna.2023.114535.
9. F. Atabiq, M. A. Wildan, and M. R. Alfianto, "Rancang Bangun Sistem Pemantauan Luaran Pico Generator pada Pembangkit Listrik Tenaga Bayu Sumbu Vertikal menggunakan Arduino UNO," *J. Appl. Electr. Eng.*, vol. 5, no. 2, pp. 43–49, 2021, doi: 10.30871/jaee.v5i2.3143.
10. D. P. Prasetya, I. Sunaryantiningsih, and R. D. Laksono, "Analisis Potensi Pembangkit Listrik Tenaga Bayu (PLTB) Di Wisata Sumber Klampok Kabupaten Nganjuk," *Setup J. Keilmuan Tek.*, vol. 1, no. 2, p. 151, 2023, doi: 10.25273/setup.v1i2.17518.151-159.
11. M. Mirza, R. S. Lubis, and M. Gapy, "Pemanfaatan alternator sebagai pembangkit listrik tenaga bayu (PLTB)," *J. Komputer, Inf. Teknol. dan Elektro*, vol. 4, no. 4, pp. 19–24, 2019, Accessed: Jan. 10, 2024. [Online]. Available: https://jurnal.usk.ac.id/kitektro/article/view/14435
12. A. Z. Wafik, "ANALISIS PERSEPSI MASYARAKAT TERHADAP RENCANA PEMBANGUNAN PEMBANGKIT LISTRIK TENAGA BAYU (PLTB) DI KECAMATAN JEROWARU," *J. Ilmu Ekon.*, vol. 2, no. 1, 2023, doi: 10.59827/jie.v2i1.53.
13. B. Rachmat and I. Garniwa, "Perancangan Sistem Berbasiskan Gelombang Laut untuk Tambahan Energi Angin pada PLTB," *J. Pendidik. Tambusai*, vol. 6, pp. 13374–13381, 2022, Accessed: Oct. 11, 2024. [Online]. Available: http://download.garuda.kemdikbud.go.id/article.php?article=2842987&val=13365&title=Perancangan Sistem Berbasiskan Gelombang Laut untuk Tambahan Energi Angin pada PLTB
14. N. Q. Nawafilah, H. R. Agustapraja, and N. Purnomo, "Penerapan Sistem Hybrid Pembangkit Listrik Tenaga Angin Dan Tenaga Surya Di Desa Pataan, Kec.Sambeng, Kab.Lamongan," *J. Mandala Pengabdi. Masy.*, vol. 3, no. 2, pp. 174–180, 2022, doi: 10.35311/jmpm.v3i2.91.
15. J. A. Wulandari, . S., and . Y., "Analisis Perkembangan Pembangkit Listrik Tenaga Bayu (PLTB) Sebagai Sumber Energi Alternatif Terbarukan Di Indonesia," *J. Pendidikan, Sains Dan Teknol.*, vol. 2, no. 4, pp. 940–945, 2023, doi: 10.47233/jpst.v2i4.1303.
16. J. D. P. Ardiana, . Y., and . S., "Analisis Potensi Energi Angin sebagai PLTB di Pantai Watu Ulo Jember Menggunakan data BMKG," *J. Pendidikan, Sains Dan Teknol.*, vol. 2, no. 4, pp. 962–965, 2023, doi: 10.47233/jpst.v2i4.1313

COMPLETE
Journal of Computer, Electronic, and Telecommunication
ISSN 2723-4371, E-ISSN 2723-5912

Article

Design of Antipodal Vivaldi Antenna with Circular Load for Bandwidth Enhancement in Radar Applications

Galuh Widya Cahyaningtyas [1], Fannush Shofi Akbar [2]*, Risdilah Mimma Untsa [3], Efrilia M. Khusna[4], Tri Agus Djoko Kuntjoro[5] and Puguh Chondro Jadmiko[6]

[1-6] Telecommunication Engineering, Telkom University, Surabaya, Indonesia
[4] James Watt School of Engineering, University of Glasgow, Glasgow, United Kingdom

* Correspondence: fanushakbar@telkomuniversity.ac.id

Received: 7 November 2024; Revised: 4 December 2024; Accepted: 31 December 2024

Abstract: Radio Detection and Rangißng (RADAR) attracts a lot of attention because it has an important role in life through its various applications such as in security, navigation, transportation, telecommunications and medical applications. Ultra-wideband radar applications require accurate, high-resolution detection and good penetration capabilities. To fulfil this, the bandwidth required must be greater, resulting in a narrower pulse width. In this case, an antenna using ultra-wideband technology is needed to accommodate this. This research discusses the design of an ultra-wideband antipodal vivaldi antenna with the addition of circular loads designed to increase bandwidth in radar applications. The design and simulation in this study used CST Studio Suite 2019 software and then measured with a Vector Network Analyzer (VNA) to determine antenna performance. The results of this study show that the antenna can work at a frequency of 898.85 MHz to more than 3.2 GHz with a unidirectional radiation pattern. In addition, the gain generated in this study is 6.6 dBi, S1.1 -17.01 dB, and a bandwidth of more than 2301.15 MHz.

Keyword: Bandwidth, Microstrip Antenna, UWB, UWB Radar, Vivaldi Antenna

1. Introduction

Radar has become a very important technology in various applications such as security, navigation, transportation, telecommunications, and the medical field [1], [2]. In use, radar obtains information about objects around us by using electromagnetic waves [3]. One of the main challenges in the development of radar systems is achieving high resolution, good accuracy, and optimal penetration capability. To achieve this, ulta-wideband radar technology using a large bandwidth is needed.

Ultra-Wideband is a short-range communication system that requires large bandwidth, and according to Federal Communication Commission (FCC) regulations, an antenna is said to be UWB when the bandwidth width is greater than 20% of its centre frequency [4], [5]. With a wide bandwidth, the ulta-wideband radar pulse can provide higher time resolution, allowing the radar system to detect objects or targets with higher precision in the time domain [6], [7]. Here, antennas have an important role in transmitting and receiving radar signals, so to achieve optimal performance the type of antenna that has a conically widened patch slot. The large bandwidth and consistent directivity of this vivaldi antenna caused the antenna to be widely developed. Therefore, wideband or ultra-wideband applications are suitable for this antenna [8].

The authors propose to design and realise a microstrip antenna using antipodal vivaldi patches and adding circular weights to each antenna arm to analyse the effect of adding circular weights on

its bandwidth. The antenna's substrate material used is FR-4 Epoxy (lossy), and the designed antenna operates in the frequency range of 1.25 GHz – 2.75 GHz, following the UWB antenna specifications for UWB radar applications, which require a bandwidth of $\geq$ 20%, a gain above 3 dBi, and S1.1 value of $\leq$ -10 dB, and a unidirectional radiation pattern.

2. Literature Review

2.1. Vivaldi Antenna

The vivaldi antenna consists of thin conductor sheets placed on top of another thin conductor sheet, with a substrate layer in between [9]. The vivaldi antenna is characterised by a tapered slot patch width, a wide bandwidth, and consistent directivity [10]. Therefore, it is suitable for wideband or ultra-wideband applications [11].

2.1.1. Conventional Antipodal Vivaldi Antenna

The antipodal vivaldi antenna is a type of antenna designed to support a wide frequency range, particularly in radar and wireless communication applications. This antenna is known for its wide radiation pattern and responsiveness to high frequencies. Its design features antipodal elements shaped like open hands, with ends that diverge, forming a ''V" shape as shown in Figure 1, which is a characteristic feature. This structure allows the antipodal vivaldi antenna to produce an excellent radiation pattern for capturing and transmitting signals across various frequencies [4]. W_{sub} is the width of the substrate, and l_{sub} is the length of the substrate. In the design of this conventional antipodal vivaldi antenna, the substrate width value is adjusted to match the width of the antenna patch ($w = W_{sub}$). To calculate the patch width, the following Equation 1 can be used [8]:

$$w = \frac{c}{2f_0\sqrt{\frac{\varepsilon_r + 1}{2}}} \tag{1}$$

Where c is the speed of light (3.10^8 m/s), f_0 is the frequency used, and ε_r is the dielectric constant used [13]. The patch length can be determined after calculating the fringing field effect for the radiating element (ΔL), as shown in Equation 2 [14]. For the effective radiating element length (L_{eff}), Equation 3 is used [8]:

$$\Delta L = 0.412h\frac{(\varepsilon_r + 0.3)(\frac{w}{h} + 0.264)}{(\varepsilon_r - 0.258)(\frac{w}{h} + 0.8)} \tag{2}$$

$$L_{eff} = l_p + 2\Delta L \tag{3}$$

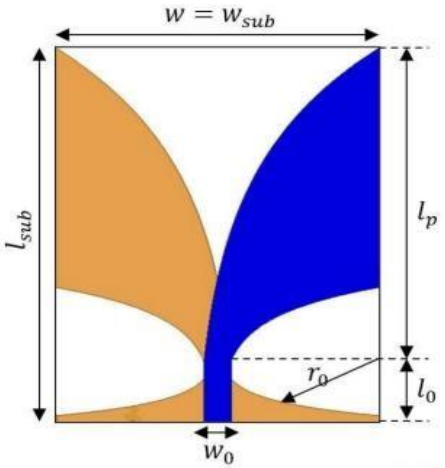

Figure 1. Conventional Antipodal Vivaldi Antenna [12]

The length of the substrate in the design of this antipodal vivaldi antenna can be determined by adding the effective radiating length of the antenna with the length of the microstrip line.

r_0 is the circular radius used by the microstrip to achieve the transition from the microstrip to the parallel strip line [1], [15]. The equation for the circular radius is [16], [17]:

$$r_0 = \frac{F}{\sqrt{1 + \frac{2h}{\pi \varepsilon_r F}\left[\ln\left(\frac{\pi F}{2h}\right)\right] + 1.7726}} \tag{4}$$

The value of r_0 is obtained using the following equation [16], [17]:

$$F = \frac{8.791 \text{ x } 10^9}{f_0 \sqrt{\varepsilon_r}} \tag{5}$$

2.2. Antipodal Vivaldi Antenna with Circular Loads

The shape of the circular antipodal vivaldi antenna is illustrated in Figure 2, where the yellow patch represents the top side patch, while the red patch represents the bottom side patch [15].

Circular loads are applied to each arm with a diameter d that is twice the radius of the load (r_0), and the value of r_0 can be determined using Equation 4. The centre point (x_0, y_0) and the radius of the circular load are r. The equation is formulated as follows [15]:

$$(x_0, y_0) = \begin{cases} x_0 = r_0 + d - r \\ y_0 = r_0 + \dfrac{(l - r_0)}{2} \end{cases} \tag{6}$$

$$r = \left[\frac{\frac{(l - r_0)^2}{4} + d^2}{2d}\right] \tag{7}$$

$$d = 2r_0 \tag{8}$$

The added circular load can improve the lower boundary radiation capability of a conventional vivaldi antenna and also cause the propagation current to travel further along the curve of the circular load, resulting in a wider bandwidth [15], [18].

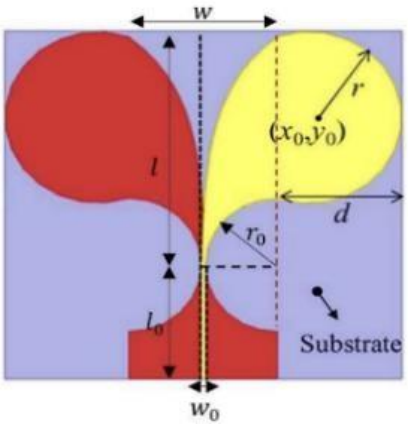

Figure 2. Antipodal Vivaldi Antenna with Circular Loads [15]

3. Antenna Design and Realisation

The specifications and design illustrations of the antenna to be developed, as well as the expected performance, can be seen in Table 1, Figure 3 and Figure 6.

3.1. Design of Conventional Antipodal Vivaldi Antenna

Based on the calculations using Equations 1, 2, 4, 6, 7, and 8, the dimensions for the antipodal vivaldi antenna are obtained, as shown in Table 2, and the design illustration of the conventional antipodal vivaldi antenna is depicted in Figure 3.

Table 1. Antenna Specifications

Specification	Value
Frequency	1.25 GHz – 2.75 GHz
S1,1	≤ −10 dB
Bandwidth	≥ 1500 MHz (≥ 75%)
Gain	≥ 3 dBi
Radiation Pattern	Unidirectional
Substrate	FR-4 Epoxy (εr = 4.3; h = 1.6)
Patch	Copper Annealed (h = 0.035)

Table 2. Design Dimensions of The Antipodal Vivaldi Antenna

Dimension	Conventional	Circular Load	Descriptions
$w_{sub} = w$	45.50 mm	288 mm	Substrate width
l_{sub}	90.00 mm	205.00 mm	Substrate length
w_p	45.50 mm	120.00 mm	Patch width
l_p	66.00 mm	189.00 mm	Patch length
l_0	24.00 mm	16.00 mm	Feeding length
w_0	13.50 mm	4.98 mm	Feeding width
r_0	21.00 mm	10.00 mm	Circular radius length
(x_0, y_0)	-	(22,24)	Centre point of circular load
d	-	184 mm	Diameter of circular load
r	-	92 mm	Radius of circular load

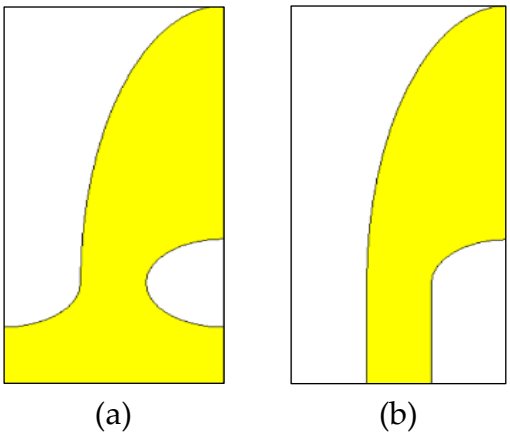

Figure 3. Design of Conventional Antipodal Vivaldi Antenna: (a) Front Side; (b) Back Side

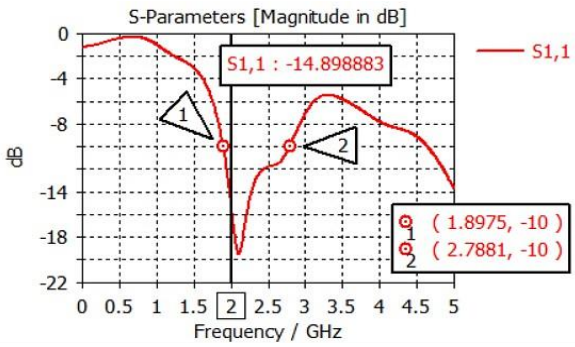

Figure 4. S1,1 and Bandwidth of the Conventional Vivaldi Antenna

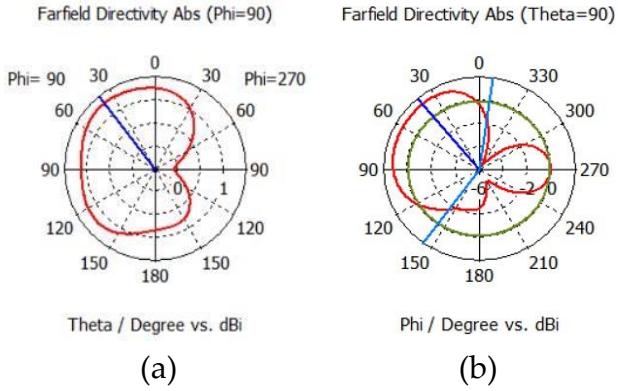

Figure 5. Radiation Pattern of the Conventional Vivaldi Antenna (f = 2 GHz): (a) E-Plane; (b) H-Plane

Based on the simulation result, the S-Parameter value within the designed frequency range meets the antenna specification standard at -14.898883 dB, as shown in Figure 4. Meanwhile, the bandwidth value complies with the FCC standard for radar and other ultre-widebandd applications, achieving 890.6 MHz (38.01%). However, this bandwidth doesn't yet meet the desired antenna specification target of over 1500 MHz or more than 75%. Additionally, the antenna gain falls below the desired specification target with a value of 1.133 dBi, as seen in Figure 5. Therefore, circular loads need to be added to each arm of the antenna to increase both the bandwidth and gain to meet the desired specifications.

3.2. Design of Antipodal Vivaldi Antenna with Circular Loads

From the conventional antipodal vivaldi antenna design, the obtained bandwidth and gain values still don't meet the target specifications. Therefore, circular loads are added to each arm of the antenna with dimensions, as shown in Table 2, and the antenna design is illustrated in Figure 6.

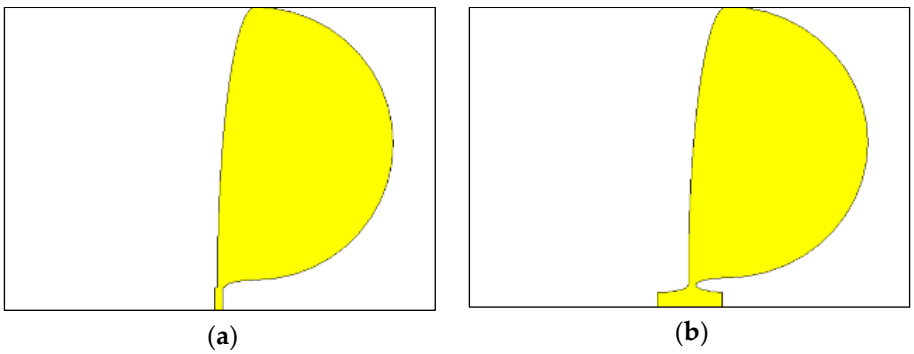

Figure 6. Design of the Antipodal Vivaldi Antenna with Circular Load: (a) Front Side; (b) Back Side

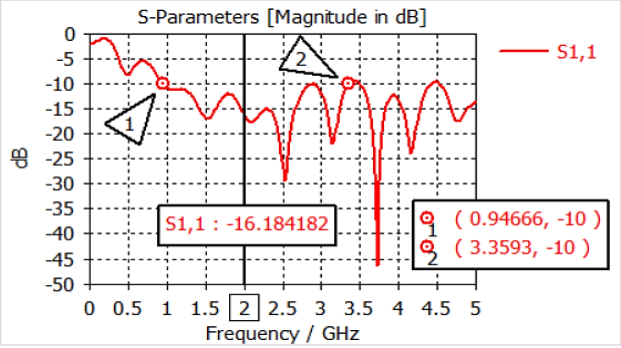

Figure 7. S1,1 and Bandwidth of the Antipodal Vivaldi Antenna

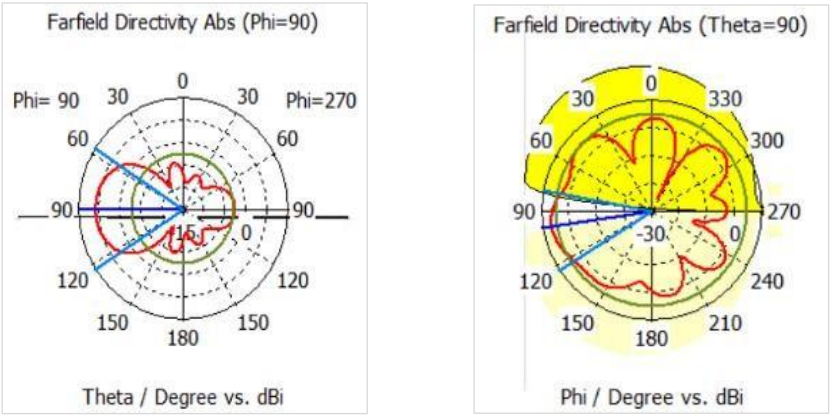

(**a**) (**b**)

Figure 8. Radiation Pattern of the Antipodal Vivaldi Antenna with Circular Loads (f = 2 GHz): (a) E-Plane; (b) H-Plane

After simulation, the S1.1 value and bandwidth within the designed frequency range meet the target at -16.184182 dB, with the bandwidth expanding from 890.6 MHz (before adding the circular loads) to 2412.55 MHz, equivalent to 112%, as shown in Figure 7. The radiation pattern of the antipodal vivaldi antenna with circular loads produces a unidirectional pattern with a gain of 5.535 dBi, as shown in Figure 8. This meets the desired antenna specification target, allowing the process to proceed to the next stage, which is antenna fabrication and performance measurement to determine the actual performance of the antenna.

3.3. Realisation of Antipodal Vivaldi Antenna with Circular Loads

The antenna that has been designed and simulated to achieve the desired reference frequency is then fabricated, as shown in Figure 9 below.

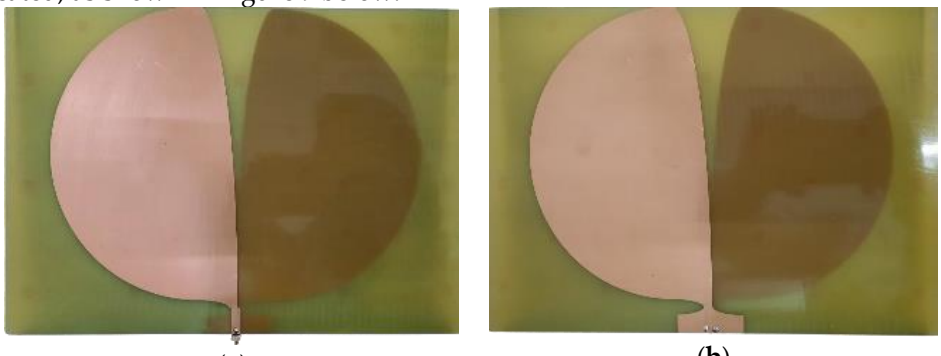

(**a**) (**b**)

Figure 9. Fabricated Antenna: (a) Front Side; (b) Back Side

4. Result and Discussion

4.1. Measurement Result of the Antipodal Vivaldi Antenna with Circular Loads

The fabricated antenna was measured for its parameters to determine the actual performance of the fabricated antenna.

The measurement results of the S-Parameter can be seen in Figure 10, where the S1,1 value is -17.01 dB, which is not significantly different from the simulated S1,1 value of -16.184182 dB. The obtained result is below -10 dB, indicating that the antenna's reflection power is comparable to the received power by the antenna [19].

In general, the higher the S1,1 value, the better the antenna is at matching its impedance, resulting in less signal power being reflected back to the source. A high S1,1 value indicates good antenna efficiency and optimal transmission performance [20]. From the measurement results, the graph shows many ripples, which can be attributed to several factors, such as the presence of other elements or structures near the antenna, non-uniformity in the antenna construction materials, especially in the PCB or antenna substrate, which can cause variations in power reflection characteristics. Additionally, changes in temperature, humidity, or other environmental factors can affect the material characteristics of the antenna, leading to variations in power reflection. Calibration factors of the VNA may also influence the measurement results.

The measurement results also showed a bandwidth of over 2301.15 MHz, equivalent to 112.28%. This exceeds the target antenna specification of at least 1500 MHz or a minimum of 75%. The achieved bandwidth represents a significant improvement compared to the conventional antenna design without circular loads.

4.2. Comparison of Bandwidth Parameters between Simulation and Measurement Result

From the simulation process of the S-Parameter for the conventional antipodal Vivaldi antenna design and the circular load design, the comparison of S-Parameter values can be seen in Figure 11. Meanwhile, the comparison of S-Parameter values between the simulation results of the Vivaldi antenna using circular loads and the measurement results of the fabricated design can be viewed in Figure 12.

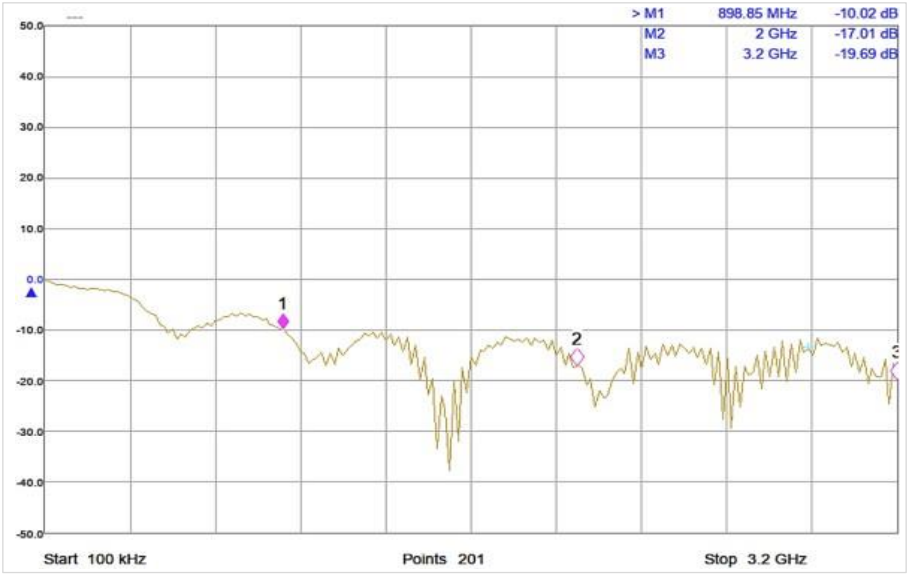

Figure 10. Measurement Result of S1,1 and Bandwidth of the Antipodal Vivaldi Antenna with Circular Loads

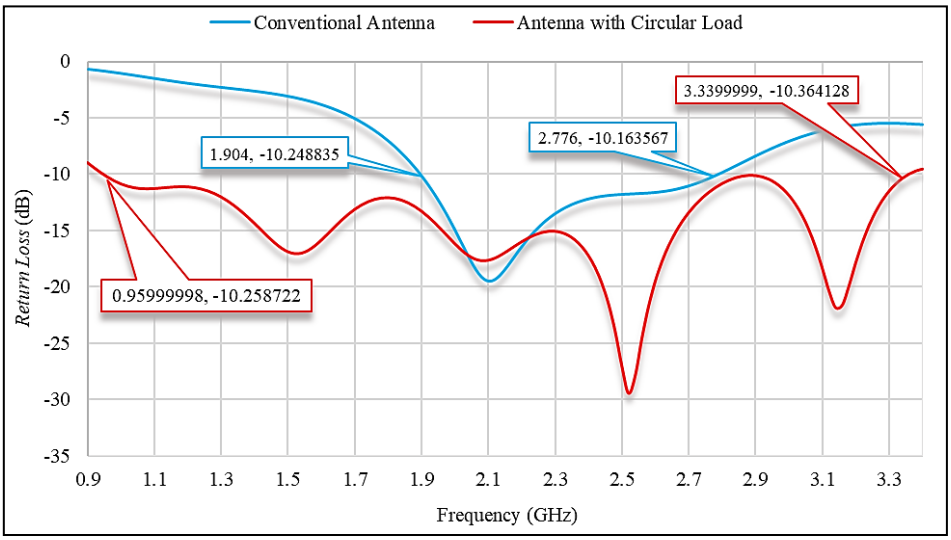

Figure 11. Comparison of Bandwidth between the Simulation Results of Conventional Vivaldi Antenna Design and The Simulation Results of Antipodal Vivaldi Antenna Design with Circular Loads

The simulation results indicate that the addition of circular loads significantly affects the bandwidth expansion. As the diameter of the circular load increases, the frequency range that constitutes the bandwidth also broadens. This frequency range expansion is illustrated in Figure 11. For the conventional antipodal Vivaldi antenna simulation, the frequency range for the bandwidth is from 1.8975 GHz to 2.7881 GHz, resulting in a bandwidth of 890.6 MHz or approximately 38.01%. Meanwhile, the simulation with circular loads shows the frequency range for the bandwidth extending from 0.94665 GHz to 3.3592 GHz, resulting in a bandwidth of 2412.55 MHz or around 112%. The bandwidth increased by 73.99% or approximately 1521.95 MHz after adding the circular load. Figure 11 also shows that the S1,1 values for both the conventional antenna design and the design with circular loads meet the S1,1 standardisation for antennas, being less than -10 dB, indicating that the antenna's reflected power is comparable to its received power.

Furthermore, from the measurement and simulation process of the S-Parameter for the circular antipodal Vivaldi antenna design, the comparison of bandwidth values is presented in Figure 12. It can be observed that the bandwidth value is 2412.55 MHz, while the measurement of the fabricated antenna yielded a bandwidth of over 2301.5 MHz, as the VNA's maximum frequency can only reach up to 3.2 GHz, equivalent to 112.28%. When comparing the simulated design with the fabricated design, the bandwidth expansion increased by over 28%.

The substantial bandwidth offers advantages for ultra-wideband radar applications, where a larger bandwidth allows ultra-wideband radar pulses to provide higher time resolution. This enables the radar system to detect objects or targets with greater precision in the time domain.

The comparison results in Figure 12 indicate that the measurement results display a ripple in the graph. This phenomenon can be attributed to several factors, such as the presence of other elements or structures close to the antenna and lack of material uniformity in the antenna construction, particularly in the PCB or antenna substrate, which may cause variations in reflection characteristics. Additionally, changes in temperature, humidity, or other environmental factors can affect the material characteristics of the antenna, leading to fluctuations in power reflection. Calibration issues with the Vector Network Analyzer (VNA) can also influence measurement results. If the equipment is not properly calibrated, discrepancies between various components, including transmitters, signal-directing elements, and receivers, will result, causing measurement results to deviate from the actual characteristics of the measured device.

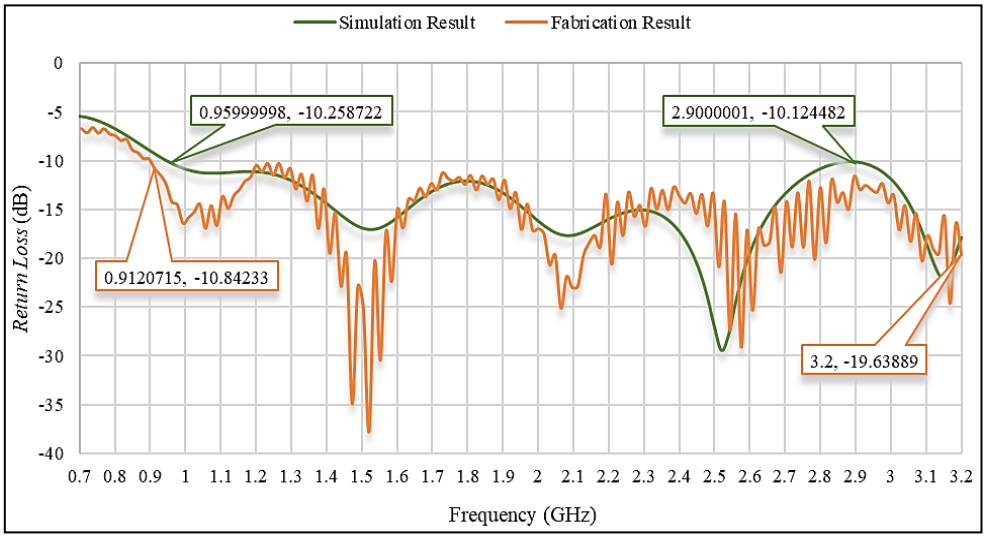

Figure 12. Comparison of Bandwidth between Simulation and Fabrication Results of Circular Antenna Vivaldi Antipodal

Such conditions are common, and in this case, optimisation to enhance antenna performance is not necessary as long as the S1,1 measurement remains within the standard performance parameter for antennas, which is less than -10 dB. However, if the S1,1 value during the measurement process exceeds -10 dB, optimisation of the antenna design and remanufacturing are required. Generally, a smaller S1,1 value (less than -10 dB) indicates better antenna performance in impedance matching and reduced signal power reflection to the source. A low S1,1 value also reflects good antenna efficiency and optimal transmission performance.

The comparison between the radiation patterns and gain of the circular antipodal Vivaldi antenna for simulation and fabrication is presented in Figure 13-(a) for the E-Plane and Figure 13-(b) for the H-Plane.

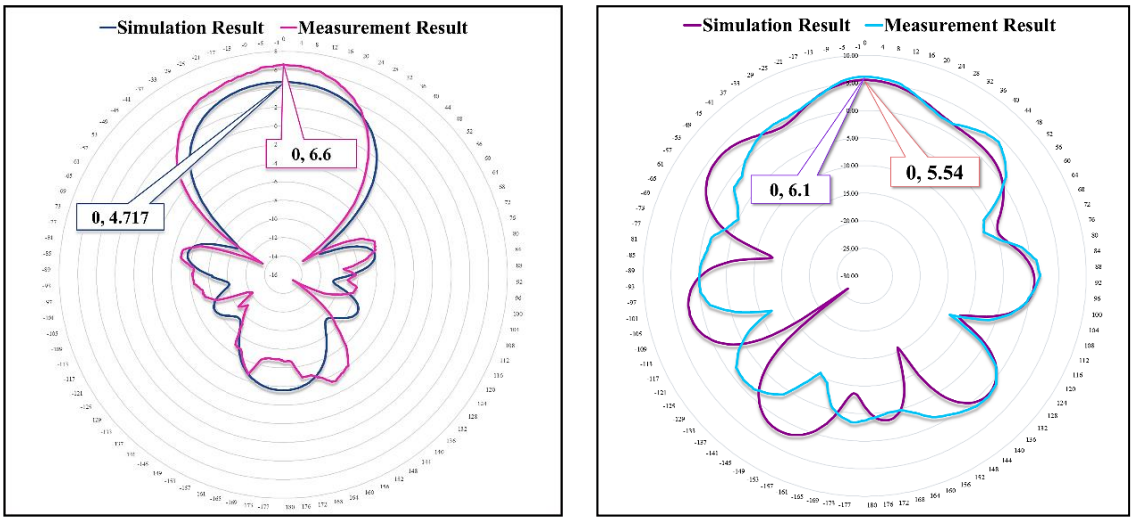

(**a**) (**b**)

Figure 13. Comparison of Radiation Pattern between Simulation and Fabrication of Antenna Vivaldi Antipodal: (a) E- Plane; (b) H-Plane

Table 3. Comparison of Antenna Parameters for the Antenna Vivaldi Antipodal Design

Antenna Parameters	Results of Antenna Vivaldi Antipodal Simulation		Results of Antenna Vivaldi Antipodal Fabrication
	Conventional	With Circular Load	With Circular
S1,1	-14.898883 dB	-16.184182 dB	-17.01 dB
Bandwidth	890.6 MHz	2412.55 MHz	≥ 2301.15 MHz
Gain	1.133 dBi	5.535 dBi	6.6 dBi
Radiation Pattern	Omnidirectional	Unidirectional	Unidirectional

The simulation results using CST Studio Suite 2019 for the radiation pattern and gain in the E-Plane show a linear directional radiation pattern with a peak gain of 4.717 dBi. During the antenna measurement, when the reference horn faced horizontally, and the test antenna faced vertically, the test antenna yielded a vertical linear directional radiation pattern with a peak gain of 6.6 dBi at 0° phi, as shown in Figure 13-(a).

The simulation results using CST Studio Suite 2019 for the H-Plane show a peak gain of 5.535 dBi. During measurement, when the reference horn antenna faced vertically, and the test antenna faced horizontally, the test antenna exhibited a horizontal linear directional radiation pattern with a peak gain of 6.1 dBi at 0° theta. The measurements in both the E-Plane and H-Plane yielded a linear polarisation with a directional radiation pattern and optimal gain of 6.6 dBi, which meets the specifications of the designed antenna.

The differences between the simulation and measurement results are due to various factors, including the fact that the antenna measurements were not conducted in a specialised or anechoic chamber, thus being affected by unwanted wave reflections from surrounding objects.

To simplify, a comparison of antenna parameters between simulation and fabrication results can be seen in Table 3 below.

5. Conclusions

The antenna can operate at frequencies from 898.85 MHz to over 3.2 GHz and achieves a measured S1,1 value of -17.01 dB with a gain of 6.6 dBi. The increase in bandwidth from the simulation results between the conventional antenna design and the design with the added circular load is 74.27%, from 890.6 MHz (equivalent to 38.01%) to 2412.55 MHz (equivalent to 112%). Meanwhile, the increase in bandwidth between the fabricated antenna design and the simulation design with the added circular load exceeds 28%, reaching more than 2301.15 MHz (equivalent to over 112.28%). This bandwidth increase is influenced by the diameter of the circular load. The larger the diameter of the circular load, the greater the bandwidth value. The resulting radiation pattern is unidirectional, which in radar applications can help direct electromagnetic wave energy in a specific direction, as well as enhance angular resolution and the ability to detect and distinguish targets with high precision.

References

1. M. A. Saputra, H. Wijanto, and Y. Wahyu, "Ultra Wideband (UWB) Circular Antipodal Vivaldi Antenna for Wall-Penetrating Radar," *National Seminar on Science and Technology, Faculty of Engineering, Universitas Muhammadiyah Jakarta*, vol. 17, Oct. 2018.
2. N. Nurhayati, A. M. De Oliveira, M. N. B. M. Yasin, and D. Kurniawan, "Palm Tree Coplanar Vivaldi Antenna Array on the Same Substrate Size: Design and Performance Evaluation," *International Journal of Electronics and Communications Systems*, vol. 2, no. 2, pp. 57–63, Dec. 2022, doi: 10.24042/ijecs.v2i2.14221.
3. M. Skolnik, *Radar Handbook*, Third Edition. The McGraw-Hill Companies, 2008.
4. M. A. Noval, Nurhayati, L. Anifah, and Rr. H. P. A. Tjahyaningtijas, "Wibeband Vivaldi Coplanar Antenna Design for Through-Wall Radar (TWR) Applications," *Journal of Electrical Engineering*, vol. 12, no. 1, pp. 9–18, 2023.

5. Editorial Teams, "What Are UWB?," Everything RF. Accessed: Jun. 29, 2023. [Online]. Available: https://www.everythingrf.com/community/what-are-uwb-radars
6. N. S. Hasim *et al.*, "Erratum to 'A Slotted UWB Antipodal Vivaldi Antenna for Microwave Imaging Applications' A Slotted UWB Antipodal Vivaldi Antenna for Microwave Imaging Applications," 2019.
7. D. R. Mandalika, D. Arseno, and Y. P. Saputera, "Design and Realisation of Ultra Wideband Vivaldi Antenna for Soil Water Content Radar," *Journal Of Electrical And System Control Engineering*, vol. 5, no. 2, pp. 59–69, Feb. 2022, doi: 10.31289/jesce.v5i2.5774.
8. Constantine. A. Balanis, *Antenna Theory Analysis and Design Fourth Edition by Constantine A. Balanis*, Fourth Edition., vol. Fourth Edition. John Wiley & Sons, Ins., Hoboken, New Jersey, 2016.
9. M. Risyad Azhary, H. Wijanto IrMT, and Y. S. Perdana, "Vivaldi Microstrip 2x2 Array Antenna for 3-6 GHz Ultra-Wideband Respiratory Detection."
10. R. Rianza *et al.*, "Conventional Vivaldi Antenna for Application in Weather Radar (9.4 GHz)," *Electrons: Scientific Journal*, pp. 1–6, Jun. 2022, doi: 10.30630/eji.14.1.236.
11. R. Arie Sadewa Setiyanto, R. Roro Hapsari Peni Agustin Tjahyaningtijas, and L. Rakhmawati, "Application of Vivaldi Antipodal Antenna for Ground Penetrating Radar by Using B-Scan Method."
12. A. S. Dixit and S. Kumar, "The enhanced gain and cost-effective antipodal Vivaldi antenna for 5G communication applications," *Microw Opt Technol Lett*, vol. 62, no. 6, pp. 2365–2374, Jun. 2020, doi: 10.1002/mop.32335.
13. A. Y. Putranto *et al.*, "Design of Circular Patch Microstrip Antenna with Inset-Feed and Array at 3.5 GHz Frequency for 5G Communication System."
14. D. Latika Herda *et al.*, "Design of 2-18 GHz Antipodal Vivaldi Antenna for Radio Direction Finder," 2023.
15. M. Alief, F. Amin, and H. Wijanto, "Vivaldi Array Microstrip Antenna at X-Band for Wall-Penetrating Radar," *TELKATIKA*, vol. 1, no. 2, p. 55, 2022.
16. B. B. Harianto, N. Pambudiyatno, P. Asih, B. Junipitoyo, and P. P. Surabaya, "Circular Patch Microstrip Antenna Design Using Insert Feeding at L-Band Frequency for PSR Applications," 2020.
17. N. Olivia and H. Wijanto, "Design and Realisation of 5.8 GHz Circular Patch Microstrip Antenna for ADS-B Data Downlink."
18. J. Bai, S. Shi, and D. W. Prather, "Modified compact antipodal Vivaldi antenna for 4-50-GHz UWB application," *IEEE Trans Microw Theory Tech*, vol. 59, no. 4 PART 2, pp. 1051–1057, Apr. 2011, doi: 10.1109/TMTT.2011.2113970.
19. Herudin. "Design of a 2.6 Ghz Microstrip Antenna for LTE (Long Term Evolution) Applications." SETRUM, vol. 1, No. 1, p.43, Jun. 2012, ISSN:2301-4652.
20. J. Guo, J. Tong, Q. Zhao, J. Jiao, J. Huo, and C. Ma, "An Ultrawide Band Antipodal Vivaldi Antenna for Airborne GPR Application," *IEEE Geoscience and Remote Sensing Letters*, vol. 16, no. 10, pp. 1560–1564, Oct. 2019, doi: 10.1109/LGRS.2019.2905013.

COMPLETE
Journal of Computer, Electronic, and Telecommunication
ISSN 2723-4371, E-ISSN 2723-5912

Article

A Mobile App for Counting Shrimp Larvae Based on the YOLO V5 Method

Shochibah Yatimatul Asmak [1], Denny Daffa Rizaldi [2], Rendy Adi Fatma Saputra [3], Anan Pepe Abseno [4], Valentinus Roby Hananto [5, 7] and Eka Sari Oktarina [6]*

[1] Department of Computer Engineering, Universitas Dinamika, Surabaya, Indonesia
[2-3] Department of Information System, Telkom University Surabaya, Surabaya, Indonesia
[4] Department of Digital Manufacturing, Indonesia Multi Colour Printing, Krian, Indonesia
[5] College of Information Science and Engineering, Ritsumeikan University, Ibaraki, Japan
[6] Department of Computer Engineering, Telkom University Surabaya, Surabaya, Indonesia
[7] Department of Information Systems, Universitas Dinamika, Surabaya, Indonesia

* Correspondence: ekasario@telkomuniversity.ac.id

Received: 6 December 2024; Revised: 13 December 2024; Accepted: 31 December 2024

Abstract: Manual counting of shrimp larvae in aquaculture is labour-intensive and time-consuming. This study aims to develop a mobile application to automate the counting process using an object detection algorithm. The application features dual functionality for real-time camera capture and image upload. Model performance was evaluated using several metrics, including Mean Average Precision, precision, and recall. The object detection model achieved a Mean Average Precision (mAP) of 93.93%, precision of 91%, and recall of 89.3%. Trials of the application demonstrated an average accuracy rate of 91.03% in detecting shrimp larvae. Despite challenges in detecting transparent larvae and distinguishing them from debris, the results indicate that the application holds promise for enhancing efficiency in shrimp farming operations. Future improvements may be directed towards enhancing application performance by refining the dataset and tuning model parameters to increase recall without compromising precision. This study represents a significant step towards integrating AI-driven technologies into aquaculture, potentially transforming the shrimp larvae counting and management process in the industry.

Keywords: Counting Larva, Object Detection, Shrimp Larvae

1. Introduction

Brackish-water cultivation is widely used in Indonesia. Shrimp aquaculture is one of these. Indonesia's shrimp farming contributes to its foreign exchange, and it is the fourth largest exporter after India, Ecuador, and Argentina [1]. There are two main activities in shrimp farming: seeding and rearing [2]. The effectiveness of shrimp production relies not only on environmental elements and pond management but also on the precision of calculating the quantity and quality of stocked shrimp seeds. Accurate counting of shrimp fry is crucial for aquaculture operations, as it directly impacts the potential value of the product and overall farm management. Traditional manual counting methods are time-consuming and can potentially harm fry, leading to the development of more efficient and accurate techniques [3].

Digital image processing techniques are increasingly being applied in aquaculture to count and detect larvae, offering significant advantages over traditional manual methods. These techniques utilize computer vision and deep learning algorithms to automate the process, thereby improving the efficiency and accuracy of fish farming operations [5] [6]. Deep learning-based object detection techniques have shown promising results for simultaneously classifying and localizing fish of interest

in images and videos [5]. For instance, in [8], a combination of canny edge detection techniques and clump analysis was used to count shrimp larvae. The results indicated that the proposed method achieved a Root Mean Square Error (RMSE) value of less than 6%, outperforming manual counting methods. Shrimpseed on [5], a modified CSRNet convolutional neural network, achieved higher accuracy in shrimp seed counting. The results showed that after only 50 iterations, the average absolute error of the algorithm was reduced to 17.28, with an accuracy rate of 95.53%. Other research [10] applied image segmentation, edge detection, and unsupervised machine learning methods to the Raspberry Pi Zero W. This system exhibits satisfactory speed to complete the calculation in one second and a high accuracy of 96%. Armavilia et al. [2] used YOLOv3 to automatically count shrimp larvae. The results of the YOLOv3 final model show a good performance with a mean Average Precision (mAP) value of 96.83% and an average accuracy value of 76.48%. Light-YOLOv4 exhibited better comprehensive performance in terms of counting accuracy, model size, and detection speed.

We used YOLOv5 to count the number of shrimp larvae in this study. A study by Wibowo et al. (2023) demonstrated the application of YOLOv5 for detecting fresh and spoiled fruit. In this experiment, YOLOv5 was used to automatically classify fruit as either fresh or spoiled, achieving excellent performance in terms of both speed and accuracy. YOLOv5 was able to classify fruit with high accuracy, which could significantly enhance the efficiency of fruit selection processes in the agricultural industry [11]. The success of YOLOv5 in detecting fresh and spoiled fruit further reinforces its suitability for other object detection tasks, such as shrimp larvae detection or agricultural pest identification. In this study, we counted the larvae using two methods: real-time using a camera accessed through an Android application installed on a smartphone or by uploading an image to the application.

2. Materials and Methods

The study described focuses on developing a mobile application for detecting and counting shrimp larvae using the YOLOv5 algorithm. This innovative approach combines advanced computer vision techniques with mobile technology to create a practical tool for aquaculture professionals. The system framework, as illustrated in Figure 1, outlines the key components and processes involved in the application's functionality.

The data collection process utilizes a high-quality Yi Camera, capable of capturing images at 16 megapixels and recording video at 60 frames per second. This ensures that the input data is of sufficient quality for accurate detection and counting of shrimp larvae. The research methodology comprises three main stages: data image collection and annotation, data training, and system testing. The image collection and annotation phase likely involves gathering a diverse set of shrimp larvae images and manually labeling them to create a robust dataset. This annotated dataset is then used to train the YOLOv5 model, which is known for its efficiency in real-time object detection tasks. Finally, the system undergoes testing to evaluate its performance and accuracy in detecting and counting shrimp larvae under various conditions, potentially including different lighting, water clarity, and larval densities.

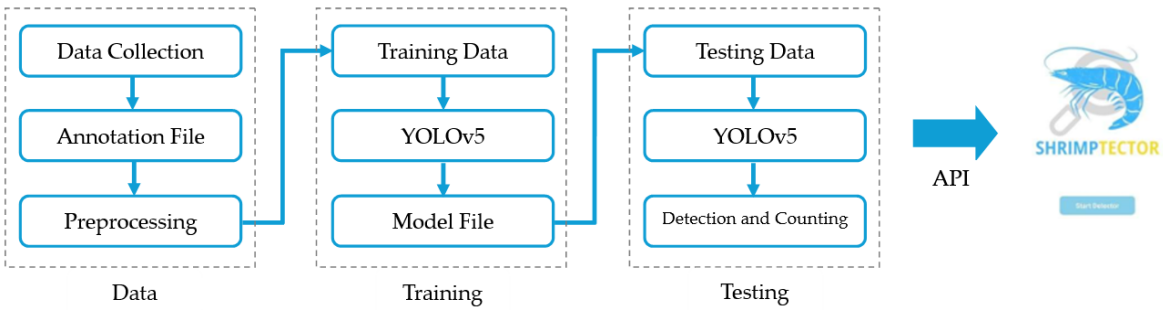

Figure 1. System Framework

2.1. Data Collection

Data collection for this research was conducted at the Banjar Kemuning Brackish Water Aquaculture Fisheries Center in Sidoarjo, East Java. The study focused on 5,000 shrimp larvae, specifically those in the PL 8 to PL 12 stages. A Yi camera was employed to capture images of these larvae, producing photographs in JPG format. The experimental setup involved placing the larvae in a white container with a water depth of 1.5 cm. The camera was positioned 20 cm above the container, and images were captured without any specific consideration for lighting conditions, as shown in Fig. 2.

The image acquisition process followed a systematic approach to create a comprehensive dataset. The larvae were divided into groups of increasing sizes, starting with ten larvae per container and progressively increasing to 20, 30, and so on, up to a maximum of 100 larvae per container. The larvae utilized were between 8 to 12 days old (PL8-PL12). Multiple photographs were taken for each group size. This methodical approach allowed for the creation of a diverse dataset that captured various densities of shrimp larvae, as illustrated in Fig. 3. The resulting dataset provides a valuable resource for analyzing shrimp larvae at different population densities, potentially aiding in the development of automated counting or monitoring systems for aquaculture applications.

Upon completion of the image acquisition process, the next step is to perform manual annotation. The annotation process is a crucial step in data processing for training object detection models such as YOLOv5. This process aims to label the shrimp larvae present in the images, enabling the model to effectively learn the patterns and positions of the larvae. The next step involves processing the annotated image results to ensure that the data is prepared for the model training phase. Detecting transparent larvae and distinguishing them from debris using YOLOv5 presents significant challenges, as the larvae possess transparent characteristics and shapes that closely resemble the background, while the debris can exhibit a wide range of colours and forms. To address the difficulty of differentiating transparent objects such as larvae from the background or other objects like debris, we incorporated several parameters into the preprocessing and augmentation stages. The images were resized to a "Fill (with centre crop)" in 640x640 pixels. For "Auto-Adjust Contrast", we opted for "Using Adaptive Equalization" and subsequently applied a grayscale transformation to enhance the image quality. In the augmentation stage, we incorporated a parameter for "90° Rotate", allowing for both clockwise and counter-clockwise orientations. Additionally, we adjusted the saturation levels within a range of -14% to +14% and modified the brightness settings between -5% and +5%.

Figure 2. Acquisition Data

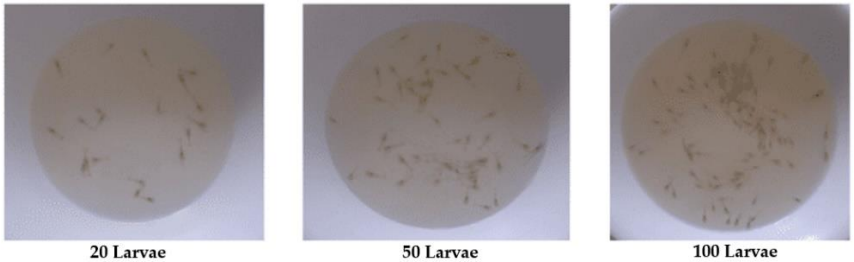

Figure 3. Group of Larvae Dataset

2.2. Training Data

The data training process is a fundamental step in the training of object detection models, wherein the model is trained using annotated data to recognize patterns and characteristics of the larvae.

This training process necessitates the availability of a well-prepared annotated dataset and the appropriate configuration of the algorithm employed for data training, which in this case is YOLOv5. YOLOv5 is a highly efficient object detection algorithm that processes input images and outputs bounding boxes containing the detected objects' locations, along with class probabilities [11][12]. One of the main advantages of YOLOv5 over earlier models is its ability to predict multiple bounding boxes and class probabilities simultaneously, all within a single neural network pass [14]. In a training experiment to detect shrimp larvae in stages PL 8 – PL 12, YOLOv5 was applied with 500 training iterations. The detection system relies on reusing classifiers or locators to perform detections, applying patterns at various positions and scales, with the best-performing areas considered as detection zones [13]. This method demonstrated high accuracy in detecting shrimp larvae, showing that YOLOv5 is particularly suited for real-time object detection tasks.

One major distinction between YOLOv5 and traditional CNNs is that YOLOv5 requires significantly fewer datasets for training. CNNs, by contrast, typically demand larger datasets and more training iterations to achieve comparable accuracy. YOLOv5 accelerates both the training process and the detection task, allowing faster and more efficient real-time processing of images [12]. This advantage makes YOLOv5 particularly well-suited for applications that require quick and accurate object detection, such as the identification of fresh and spoiled fruit or the detection of shrimp larvae.

YOLOv5 is a mature algorithm among target recognition algorithms which has the advantages of being lightweight and having a fast inference ability [16], as demonstrated in the study conducted by Babila et al. successfully implemented the YOLOv5 algorithm for detecting and inventory counting of stock, achieving an accuracy of up to 93% [17]. That study demonstrates a higher accuracy compared to previous research that utilized YOLOv3 and Light-YOLOv4. Another study by S. Gupta et al. utilized YOLOv5 for real-time object detection in surveillance videos, demonstrating its effectiveness and precision in identifying multiple object categories [18]. These studies highlight the successful implementation of YOLOv5 across various domains, including the detection of smaller objects within automotive contexts, where the YOLOv5 series has achieved commendable accuracy [19]. This indicates the algorithm's versatility and robust performance.

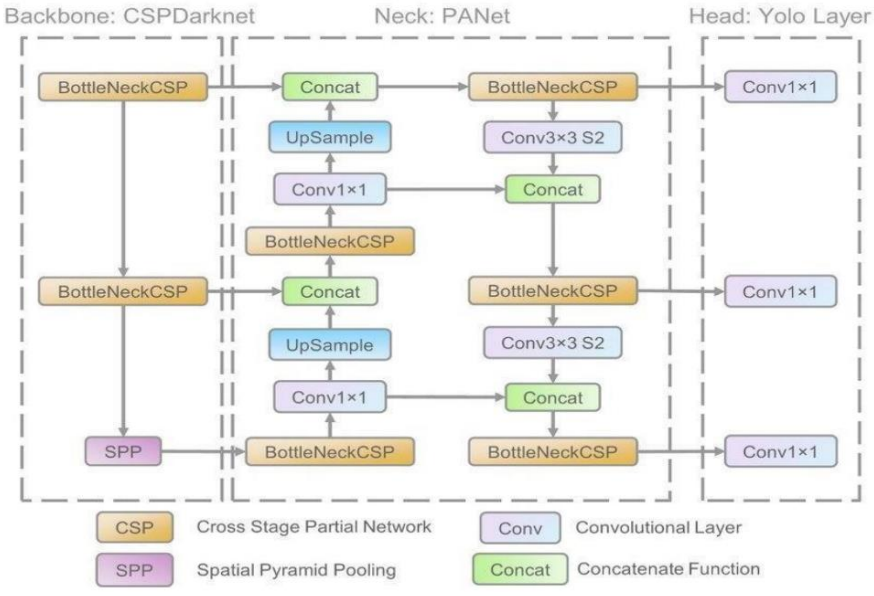

Figure 3. Network Architecture YOLOv5 [1]

2.3. Testing

The model evaluation is the next step or stage, which is conducted to see the accuracy value of the training process results on the dataset. This stage is important in detecting objects because stable object detection has a high accuracy value. For this reason, the accuracy value in object detection needs to be evaluated so that object detection has a more stable accuracy value on each image or video [2].

The detection result is the output of the entire process that has been carried out, where the results that have been detected for an object will be accompanied by an accuracy value. This stage will not occur if one of them is not run in the test framework stage. To determine the accuracy value in this study, the author uses an equation like the equation below:

$$\text{Accuracy} = \frac{\text{TP+TN}}{\text{TP+TN+FP+FN}} \text{ x } 100\%, \quad (1)$$

2.4. Mobile Application

The "Shrimp Tector" application represents a significant advancement in aquaculture technology, offering shrimp farmers a practical and efficient tool for larvae counting. By leveraging a React-based framework, the application ensures cross-platform compatibility and a smooth user experience. The dual-frame design, featuring an initial interface and a dedicated counting process frame, streamlines the workflow for farmers. This intuitive layout allows users to quickly navigate between different functionalities, enhancing overall usability.

The application's flexibility in image capture methods is particularly noteworthy, as it addresses the diverse needs of farmers operating in various environments. The option to either take a photo directly or select an image from the device's gallery caters to different preferences and situations. Moreover, the inclusion of an offline data collection feature demonstrates a thoughtful approach to real-world challenges, such as unreliable internet connectivity in remote farming locations. This feature allows farmers to capture images when convenient and process them later, ensuring that the application remains useful even in areas with limited network access. The server-side processing of images, coupled with the application's ability to interpret and display results, showcases the seamless integration of advanced object detection technology with a user-friendly interface, making complex larvae counting tasks accessible to farmers without specialized technical knowledge.

The application has been implemented in IBAP Banjarkemuning through community service conducted by Oktarina et al. According to the results of the questionnaire survey, staff and employees responded with "strongly agree" and "agree" to all questions posed. The percentage of "strongly agree" responses ranged from a maximum of 100% to a minimum of 80%. Conversely, the "agree" response rate was highest at 20% and lowest at 10% [20].

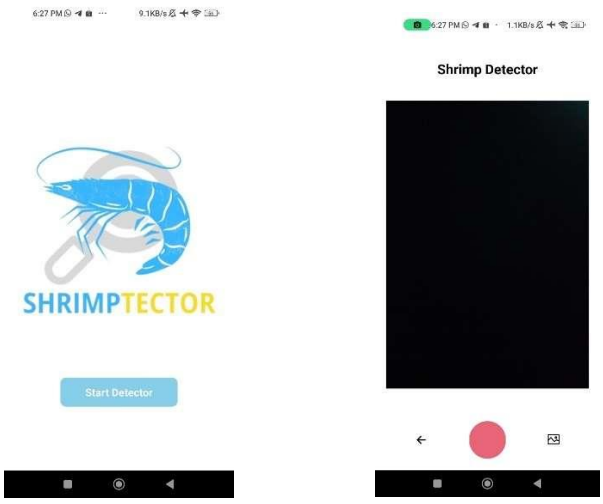

Figure 4. Shrimptector Mobile Application

3. Results

The dataset for training the YOLO model consisted of 811 images for training (70%), 232 for validation (20%), and 116 for testing (10%). The training process utilized 500 iterations with a learning rate of 0.001 and was conducted using Google Colab. The annotation process, crucial for object detection, was performed using YOLO mark tools. To enhance YOLO's performance in recognizing shrimp larvae, each image was divided into four parts. This resulted in a total of 1159 annotations across the dataset, with image sizes ranging from 0.03 MP to 15.93 MP and a median resolution of 3120 x 3456.

3.1. Annotation Image

The annotation task for detecting shrimp eyes and larval black dots was complicated by several factors inherent to the nature of the specimens and imaging conditions. The transparency of shrimp larvae posed a significant challenge, as it made distinguishing the organisms from their surroundings difficult. This was further exacerbated by the presence of debris in the samples, which could easily be misidentified as shrimp, leading to potential false positives. The dynamic nature of the larvae during image capture introduced another layer of complexity, as their movement often resulted in blurred images that obscured key identifying features. This blurring effect made it particularly challenging to accurately locate and annotate the eyes and black dots, potentially leading to missed detections or inaccurate placements.

The issue of stacked shrimp presented a unique challenge in the annotation process, as it led to inconsistencies in larval detection. In cases where multiple shrimp overlapped, the annotators faced difficulties in accurately identifying and marking individual larvae. This resulted in variable outcomes, where sometimes two larvae were detected, other times only one was identified, and in some instances, none were recognized at all. These inconsistencies highlight the complexity of the annotation task and the need for robust guidelines and possibly advanced imaging techniques to improve accuracy. The impact of these challenges on annotation accuracy is clearly demonstrated in Figure 5 (a) and (b), which provides a visual representation of the distribution of accuracy levels across the annotations. This distribution reflects the varying degrees of difficulty encountered in different images, with factors such as image quality, larval positioning, and the presence of confounding elements contributing to the observed range of accuracy levels. After enhancing the quality of the dataset through the addition of parameters during preprocessing and augmentation, the accuracy level has improved.

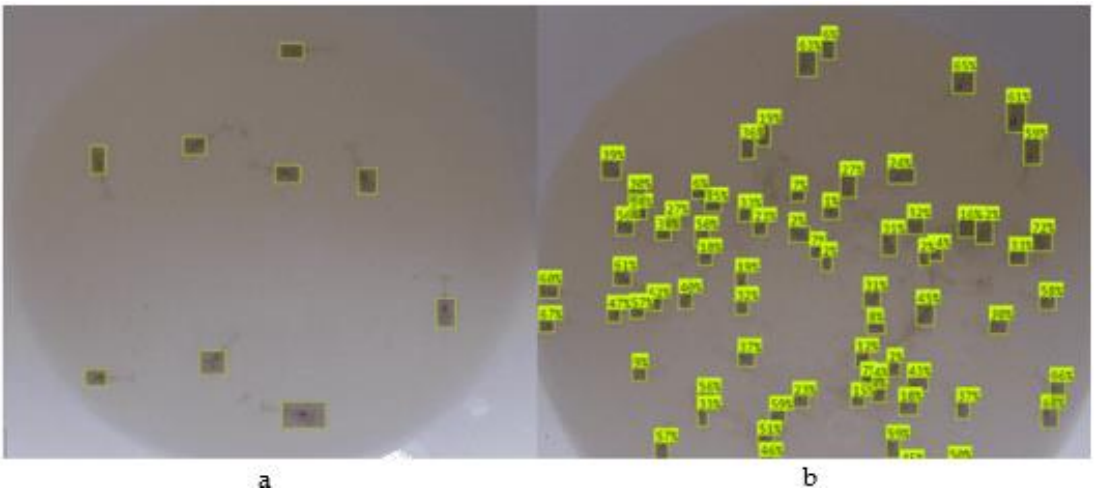

Figure 5. Annotation Process (a) small number and (b) large number

3.2 Training the Models

The data annotation is a crucial step in preparing the dataset for object detection model training. Once completed, the annotated dataset is imported into Roboflow, a platform that streamlines the machine learning workflow. Configuring the dataset in Roboflow using the prepared API key ensures seamless integration with the subsequent steps of the process. The choice of YOLOv5, for instance, segmentation [11], is significant, as it represents a state-of-the-art approach in object detection, offering a balance between speed and accuracy.

The training process for the object detection model involves fine-tuning various parameters to optimize performance. The author's decision to set the confidence threshold at 30% indicates a balance between detecting objects with reasonable certainty while minimizing false positives. Similarly, the overlap threshold of 30% helps manage instances where multiple bounding boxes may overlap for a single object. The training duration of 100 epochs suggests a comprehensive approach, allowing the model sufficient iterations to learn from the dataset and improve its accuracy. These carefully chosen parameters and the structured training process aim to produce a robust object detection model capable of accurately identifying and segmenting instances within images.

3.3 Testing

The evaluation of the trained model reveals promising results in terms of its performance metrics. The Mean Average Precision (mAP) value of 93.93% indicates a strong overall accuracy in detecting and classifying shrimp larvae across various scenarios. This metric takes into account both precision and recall, providing a comprehensive measure of the model's effectiveness. The precision value of 91% indicates a strong capability in minimizing false positive detections. Meanwhile, the recall value of 89.3% demonstrates that this model is proficient in identifying the majority of larvae present in the images. However, there remain a few undetected objects (false negatives), which could be attributed to factors such as overlapping larvae, poor lighting conditions, or the small size of the larvae. Based on the data presented in Table 1, it can be concluded that the model consistently demonstrates a high level of predictive accuracy. Among the 30 images tested, the prediction accuracy ranged from 84.00% to 96.00%. The highest accuracy of 96.00% was achieved for images 14 and 23, while the lowest accuracy was recorded for image 15 at 84.00%.

In general, a majority of the images exhibited an accuracy exceeding 90%. However, there were several outliers with lower accuracy, specifically for images 4, 15, and 20. This discrepancy may be attributed to factors such as uneven lighting, overlap among larvae, or variations in larvae size. Nevertheless, for images containing a larger number of larvae (≥60), the model maintained commendable performance with an accuracy above 85%, indicating its scalability concerning a greater number of objects. The average accuracy across all trials was 91.03%, suggesting that the YOLOv5 model is sufficiently reliable for use in automated larvae counting applications. It is advisable to retrain the model using a more diverse dataset and to implement preprocessing techniques aimed at improving image quality. Additionally, conducting trials with supplementary datasets under varying environmental conditions is recommended to assess the model's generalization capabilities. These testing results indicate that YOLOv5 holds significant potential for practical implementation in the aquaculture sector, thereby improving both efficiency and accuracy in larvae counting processes.

Table 1. Detail Accuracy of the Model

Image	Prediction	Manual	Accuracy
1	8	9	88,89%
2	8	9	88,89%
3	8	9	88,89%
4	17	20	85,00%
5	19	20	95,00%
6	19	20	95,00%
7	27	30	90,00%
8	28	30	93,33%
9	28	30	93,33%
10	36	40	90,00%
11	37	40	92,50%
12	38	40	95,00%
13	45	50	90,00%
14	48	50	96,00%
15	42	50	84,00%
16	56	60	93,33%
17	55	60	91,67%
18	54	60	90,00%
19	64	70	91,43%
20	60	70	85,71%
21	63	70	90,00%
22	74	80	92,50%
23	76	80	95,00%
24	72	80	90,00%
25	80	90	88,89%
26	81	90	90,00%
27	84	90	93,33%
28	83	90	92,22%
29	80	90	88,89%
30	83	90	92,22%

4. Conclusions

This research developed a mobile application called "Shrimp Tector" to count shrimp larvae using the YOLOv5 algorithm. The system offers two methods for image capture: real-time using a smartphone camera or uploading an image. The model achieved a Mean Average Precision (mAP) of 93.93%, a precision of 91%, and a recall of 89.3%. The application demonstrated an average accuracy of 91.03% from 30 trials, indicating its potential to facilitate and expedite the counting process for shrimp farmers. However, despite the relatively high values of precision and recall, there is a notable difference between precision and recall values (91% vs. 89.3%). This indicates that the model is slightly more focused on avoiding false positive detections rather than capturing all existing objects. To achieve a better balance, adjusting the detection threshold or retraining the model with a larger dataset that encompasses diverse environmental conditions could be considered.

Integrating this application into actual shrimp farming operations has the potential to enhance both efficiency and accuracy in the monitoring of shrimp larvae. However, it is essential to consider various challenges, including technical, operational, and user adoption aspects. It is crucial to implement technical adjustments such as improving dataset quality, utilizing superior hardware, optimizing models, and providing user training to ensure that the application functions efficiently and effectively in real-world conditions. Future work may focus on enhancing model performance through improvements in the dataset and tuning model parameters to increase recall without

compromising precision while also expanding its capabilities to accommodate various developmental stages of shrimp larvae.

References

1. P. J. G. Henriksson, L. K. Banks, S. K. Suri, T. Y. Pratiwi, N. A. Fatan, and M. Troell, "Indonesian aquaculture futures-identifying interventions for reducing environmental impacts," Environmental Research Letters, vol. 14, no. 12, 2019, doi: 10.1088/1748-9326/ab4b79.
2. S. Armalivia, Z. Zainuddin, A. Achmad, and Muh. A. Wicaksono, "Automatic Counting Shrimp Larvae Based You Only Look Once (YOLO)," in 2021 International Conference on Artificial Intelligence and Mechatronics Systems (AIMS), IEEE, Apr. 2021, pp. 1–4. doi: 10.1109/AIMS52415.2021.9466058.
3. S. Arsad et al., "The Application of Microalgae Feeding Regime on Whiteleg Shrimp Culture in Each Stage: A Mini Review," Sains Malaysiana, vol. 52, no. 1, pp. 1–16, Jan. 2023, doi: 10.17576/jsm-2023-5201-01.
4. J. Reis, A. Weldon, P. Ito, W. Stites, M. Rhodes, and D. A. Davis, "Automated feeding systems for shrimp: Effects of feeding schedules and passive feedback feeding systems," Aquaculture, vol. 541, p. 736800, Apr. 2021, doi: 10.1016/j.aquaculture.2021.736800.
5. H. Liu, L. Hao, X. Ma, Y. Yu, and L. Wang, "Application of Deep Learning-Based Object Detection Techniques in Fish Aquaculture: A Review," Journal of Marine Science and Engineering, vol. 11, no. 4, p. 867, Apr. 2023, doi: 10.3390/jmse11040867.
6. L. Zhang, W. Li, C. Liu, X. Zhou, and Q. Duan, "Automatic fish counting method using image density grading and local regression," Computers and Electronics in Agriculture, vol. 179, p. 105844, Oct. 2020, doi: 10.1016/j.compag.2020.105844.
7. X. Peng, T. Zhou, Y. Zhang, and X. Zhao, "Automatic Shrimp Fry Counting Method Using Multi-Scale Attention Fusion," Sensors, vol. 24, no. 9, May 2024, doi: 10.3390/s24092916.
8. E. A. Awalludin, M. Y. Mat Yaziz, N. R. Abdul Rahman, W. N. J. H. W. Yussof, M. S. Hitam, and T. N. T Arsad, "Combination of Canny Edge Detection and Blob Processing Techniques for Shrimp Larvae Counting," in 2019 IEEE International Conference on Signal and Image Processing Applications (ICSIPA), IEEE, Sep. 2019, pp. 308–313. doi: 10.1109/ICSIPA45851.2019.8977746.
9. D. Liu et al., "Shrimpseed_Net: Counting of Shrimp Seed Using Deep Learning on Smartphones for Aquaculture," IEEE Access, vol. 11, pp. 85441–85450, 2023, doi: 10.1109/ACCESS.2023.3302249.
10. [C.-T. Yeh and M.-S. Ling, "Portable Device for Ornamental Shrimp Counting Using Unsupervised Machine Learning," Sensors and Materials, vol. 33, no. 9, p. 3027, Sep. 2021, doi: 10.18494/SAM.2021.3240.
11. A. Wibowo, L. Lusiana, and T. K. Dewi, "Implementasi Algoritma Deep Learning You Only Look Once (YOLOv5) Untuk Deteksi Buah Segar Dan Busuk," Paspalum: Jurnal Ilmiah Pertanian, vol. 11, no. 1, p. 123, Mar. 2023, doi: 10.35138/paspalum.v11i1.489.
12. M. S. Nuha and R. Alexandro H., "Pemanfaatan Yolo untuk Pengenalan Kesegaran Buah Mangga," Joutica, vol. 7, no. 1, p. 513, Feb. 2022, doi: 10.30736/jti.v7i1.747.
13. A. Putra Pranjaya, F. Rizki, R. Kurniawan, and N. K. Daulay, "KLIK: Kajian Ilmiah Informatika dan Komputer Klasifikasi Penyakit Pada Daun Tanaman Padi Berbasis YoloV5 (You Only Look Once)," Media Online), vol. 4, no. 6, pp. 3127–3136, 2024, doi: 10.30865/klik.v4i6.1916.
14. K. Ahmad Baihaqi and C. Zonyfar, "Deteksi Lahan Pertanian Yang Terdampak Hama Tikus Menggunakan Yolo v5," Syntax : Jurnal Informatika, vol. 11, no. 02, pp. 01–11, Nov. 2022, doi: 10.35706/syji.v11i02.7226.
15. R. F. Putra and D. I. Mulyana, "Optimasi Deteksi Objek Dengan Segmentasi dan Data Augmentasi Pada Hewan Siput Beracun Menggunakan Algoritma You Only Look Once (YOLO)," Jurnal JTIK (Jurnal Teknologi Informasi dan Komunikasi), vol. 8, no. 1, pp. 93–103, Jan. 2024, doi: 10.35870/jtik.v8i1.1391.
16. Duan, H., Wang, J., Zhang, Y., Wu, X., Peng, T., Liu, X., & Deng, D. (2024). Shrimp Larvae Counting Based on Improved YOLOv5 Model with Regional Segmentation. Sensors, 24(19), 6328. https://doi.org/10.3390/s24196328

17. Babila, I. F. E., Villasor, S. a. E., & Cruz, J. C. D. (2022). Object detection for inventory stock counting using YOLOV5. IEEE 18th International Colloquium on Signal Processing & Applications (CSPA 2022). https://doi.org/10.1109/cspa55076.2022.9782028
18. Jha, S., Seo, C., Yang, E. et al., "Real time object detection and trackingsystem for video surveillance system.", Multimed Tools Appl 80, pp. 3981–3996, 2021.
19. Benjumea, A., Teeti, I., Cuzzolin, F., & Bradley, A. (2021). YOLO-Z: Improving small object detection in YOLOv5 for autonomous vehicles. arXiv (Cornell University). https://doi.org/10.48550/arxiv.2112.11798
20. Oktarina, E. S., Kusumawati, W. I., & Musayyanah, M. (2024). Implementasi Aplikasi Penghitung Benur dengan Menggunakan HP Android pada Instalasi Budidaya Air Payau Banjarkemuning, Sedati, Sidoarjo. Society Jurnal Pengabdian Masyarakat, 3(4). https://doi.org/10.55824/jpm.v3i4.427